SETTLEMENT OF EMBANKMENTS CONSTRUCTED OF UNSATURATED COMPACTED SOIL

BY

GEORGE WILLIAM ANNANDALE

A DISSERTATION SUBMITTED TO THE FACULTY OF ENGINEERING, UNIVERSITY OF THE WITWATERSRAND, JOHANNESBURG IN PARTIAL FULFILMENT OF THE REQUIREMENTS FOR THE DEGREE OF MASTER OF SCIENCE IN ENGINEERING

JOHANNESBURG

1979

DECLARATION

I, the undersigned, declare that this dissertation:

1. Is entirely my own work

2. Has not been submitted to another University for the degree of MSc(Eng).

ABSTRACT

The purpose of this investigation was to establish a method to determine settlement in compacted unsaturated soil (with special reference to embankments) by using oedometer test results.

A review of the behaviour and the principle of effective stress in unsaturated soil is given. The conclusion is reached that consolidation in unsaturated soil is largely controlled by the dissipation of excess pore-air pressure.

Methods are described to determine the soil parameters that are required to estimate pore-air pressures in unsaturated soil from oedometer tests.

A computer program is described to estimate pore-air pressures in embankments at the end of construction and at specified time intervals after completion.

A case study on the Mita Hills dam in Zambia is reported and calculated settlements of this embankment are compared with observed settlements.

Dedicated to Itha for her
encouragement and support.

ACKNOWLEDGEMENTS

The Author wishes to express his gratitude for the help given by:

1. Professor Blight, supervisor for the project, who made many useful suggestions and was always willing to discuss various problems which arose.
2. Mr G H H Legge, who was continuously interested in the project and provided the Author with the required data of Mita Hills dam.
3. The South African Council for Scientific and Industrial Research and the University of the Witwatersrand for financial support in the form of bursaries.
4. Mrs H Newey who typed the dissertation.

PREFACE

Estimating settlement of embankments requires an understanding of the volume change behaviour of unsaturated soil.

At the time when the Mita Hills dam in Zambia was designed (1956) knowledge of the behaviour of unsaturated soil was limited. It was noticed when the settlement of the crest of the dam was estimated that the oedometer curves for the unsaturated compacted soil consisted of two portions:

(i) Instantaneous compression

(ii) Consolidation compression

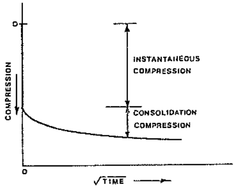

This led to the conclusion that the total settlement curve on the e:log P graph could be subdivided into an immediate and a consolidation settlement curve.

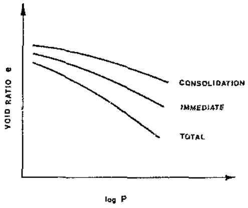

Immediate settlement occurs instantaneously as load is added, while consolidation settlement is time dependent as it is a function of the dissipation of excess pore-pressure.

Settlement of the crest of Mita Hills dam was estimated at the time by using the consolidation settlement curve and Terzaghi's classical theory for one-dimensional settlement of unsaturated soil. The consolidation settlement was estimated at 1,3 per cent of the maximum structural height and the actual settlement was 1,4 per cent.

The good correlation between actual and estimated settlement led to the decision to investigate the settlement problem by applying current concepts of the volume change behaviour of unsaturated soil.

CONTENTS | Page

CHAPTER 1

INTRODUCTION

The purpose of this dissertation was to find a method to estimate settlement in unsaturated soil without resorting to highly sophisticated laboratory testing techniques and equipment. An effort was made to evaluate all the required soil properties from the relatively unsophisticated oedometer test. The calculation of settlement was further simplified by using a modified form of the effective stress equation for unsaturated soil.

The investigation was limited to the calculation of settlements of the crests of embankment dams constructed of unsaturated compacted soil; the dissipation in two dimensions of excess pore-pressures being considered. The methods employed to estimate settlement in this dissertation can in principle be applie to other settlement problems involving unsaturated soils.

Calculations of the settlement of soil are closely linked with the principle of effective stress. Chapter 2 is devoted to a discussion of effective stress and the complex behaviour of unsaturated soil.

There are basically four methods with which settlements of soil, with special reference to embankments, can be calculated.

1.1 Empirical Formulae

These usually express settlement as a function of the height of the dam, eg:

Thomas (1976) presented the formula,

CHAPTER 1

INTRODUCTION

The purpose of this dissertation was to find a method to estimate settlement in unsaturated soil without resorting to highly sophisticated laboratory testing techniques and equipment. An effort was made to evaluate all the required soil properties from the relatively unsophisticated oedometer test. The calculation of settlement was further simplified by using a modified form of the effective stress equation for unsaturated soil.

The investigation was limited to the calculation of settlements of the crests of embankment dams constructed of unsaturated compacted soil; the dissipation in two dimensions of excess pore-pressures being considered. The methods employed to estimate settlement in this dissertation can in principle be applied to other settlement problems involving unsaturated soils.

Calculations of the settlement of soil are closely linked with the principle of effective stress. Chapter 2 is devoted to a discussion of effective stress and the complex behaviour of unsaturated soil.

There are basically four methods with which settlements of soil, with special reference to embankments, can be calculated.

1.1 Empirical Formulae

These usually express settlement as a function of the height of the dam, eg:

Thomas (1976) presented the formula,

$$S = 0{,}035\,(H-13)$$

where S = settlement at end of construction in metres

H = height of dam in metres

The formulae for settlement at 5 and 10 years after completion were given as,

$$\log S_5 = 0{,}017H - 1{,}35$$

and $$\log S_{10} = 0{,}0156H - 1{,}16$$

The above formulae were based on settlement measurements on a large number of earthfill dams in Victoria, Australia.

Settlements calculated by means of empirical formulae should only be considered as a guide to the magnitude of settlement and should not be relied upon in the final design of embankments as they do not take account of soil properties, rates of construction or geometry of the embankment. All these factors play a role in the settlement of embankments.

1.2 Numerical Evaluation of Analytical Solutions

Before settlements can be calculated using this technique an analytical solution to the specific problem under consideration must be obtained. These solutions are not always available, which makes the approach unattractive for use in practice.

Analytical solutions to estimate the pore-water pressure in a completely saturated layer of clay of infinite horizontal extent which increases in height with time are available (Gibson, 1958). These solutions consider only one-dimensional dissipation of pore-water pressures whereas the dissipation of pore-pressures in embankments is essentially two-dimensional.

Analytical solutions of this type can however be used to get a rough estimate of effective stresses in the central core beneath the crest of an embankment.

1.3 *Finite Element Technique*

This method is growing in popularity and is now used frequently. Comparisons between observed settlements and settlements calculated by finite elements can be quite good (Penman *et al*, 1971 and Duncan, 1972).

1.4 Finite Difference Technique

Solutions are obtained by writing the differential equation for consolidation in finite difference form and solving it numerically.

Gibson (1958) estimated pore-pressures in the Usk embankment dam by solving the finite difference form of the one-dimensional consolidation equation.

The finite difference form of the two-dimensional consolidation equation will be used in this dissertation to estimate pore-pressures in the embankment. If the excess pore-pressures are known it is possible to estimate both effective stresses and settlement.

The method used in this dissertation was as follows: Literature on the behaviour of and the principle of effective stress in unsaturated soil were first studied. Hence, certain conclusions were reached which enabled the effective stress in unsaturated soil to be simply approximated.

These conclusions were applied to the settlement curves obtained from oedometer tests to obtain a better understanding of the behaviour of compacted unsaturated soil in the oedometer and it was found that certain soil properties required to calculate pore-pressures in unsaturated soil can be estimated from oedometer test results.

A finite difference computer program was then developed which can be used to calculate excess pore-pressures in embankments at the end of construction and at various time intervals thereafter. The effective stress in the central core beneath the crest of the embankment can be evaluated if the excess pore-pressures are known. The settlement of the crest can then be calculated from the effective stress.

Settlements were calculated for the Mita Hills dam in Zambia and compared with observed settlements.

CHAPTER 2

VOLUME CHANGE IN UNSATURATED SOILS

2.1 Introduction

In this chapter a brief review of the principle of effective stress will be given, especially as it applies to volume change in unsaturated soils. Considerable controversy exists in literature on the applicability of the effective stress principle to volume change in unsaturated soils (see eg, Burland, 1965 and Blight, 1965). An attempt will be made to present the main schools of thought on this subject.

Terzaghi (1943) proposed the principle of effective stress for saturated soils and defined it as that stress which causes measurable changes in volume and shear strength in soils. It is a function of the total stress σ and the pore-pressure u. The effective stress in saturated soils was formulated by Terzaghi as

$$\sigma' = \sigma - u \qquad \ldots(2.1)$$

where σ' = effective stress

The opinion is often expressed that the success experienced in applying this equation to predict the behaviour (ie volume change and strength) of saturated soils actually led to the *birth* of the science of soil mechanics.

As many of the soils that engineers have to deal with are unsaturated, a series of attempts have been made to formulate a similar equation that will apply to unsaturated soils.

CHAPTER 2

VOLUME CHANGE IN UNSATURATED SOILS

2.1 Introduction

In this chapter a brief review of the principle of effective stress will be given, especially as it applies to volume change in unsaturated soils. Considerable controversy exists in literature on the applicability of the effective stress principle to volume change in unsaturated soils (see eg, Burland, 1965 and Blight, 1965). An attempt will be made to present the main schools of thought on this subject.

Terzaghi (1943) proposed the principle of effective stress for saturated soils and defined it as that stress which causes measurable changes in volume and shear strength in soils. It is a function of the total stress σ and the pore-pressure u. The effective stress in saturated soils was formulated by Terzaghi as

$$\sigma' = \sigma - u \qquad \ldots(2.1)$$

where σ' = effective stress

The opinion is often expressed that the success experienced in applying this equation to predict the behaviour (ie volume change and strength) of saturated soils actually led to the *birth* of the science of soil mechanics.

As many of the soils that engineers have to deal with are unsaturated, a series of attempts have been made to formulate a similar equation that will apply to unsaturated soils.

2.2 Qualitative Description of the Behaviour of Unsaturated Soils

Before an attempt is made to qualitatively describe the behaviour of unsaturated soils, one should first investigate the nature of these materials.

Unsaturated soil is a multi-phase continuum, consisting of four phases, ie

(i) Mineral grains

(ii) Porewater

(iii) Pore-air

(iv) Contractile skin, ie the interface between the air and water phases.

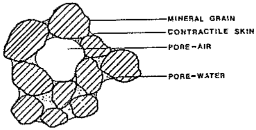

FOUR PHASES OF UNSATURATED SOIL

Figure 2.1

The mechanisms of volume change in soils will be discussed qualitatively before discussing the role of effective stress.

There are basically four mechanisms of volume change (see eg Lambe and Whitman, 1969).

2.2.1 Elastic deformation of the mineral grains

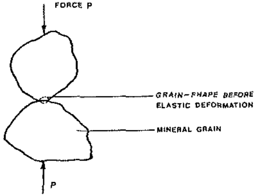

Figure 2.2

The elastic deformations of grains are very small and have only a minor effect on volume change.

2.2.2 Elastic bending of clay particles

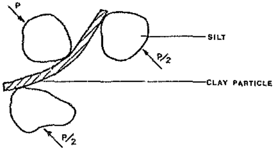

Figure 2.3

2.2.3 Slip of grains due to exceeding the frictional resistance of surfaces between grains.

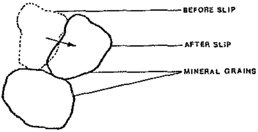

Figure 2.4

The *slip of grains* provides the major contribution to volume change in granular soils and explains why the rebound in soils when load is removed is so small. During loading the grains move to more stable, lower energy states, and will not move back to their previous positions when the load is removed as this will require additional energy which *is not* available.

2.2.4 Swelling

When clay particles absorb water they swell. Swelling is influenced by the chemical properties of the clay particles and pore fluid. This phenomenon can have a considerable effect on volume change in soils.

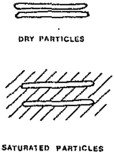

Figure 2.5

The effect of the air, water and contractile skin phases on the behaviour of unsaturated soils will now be discussed:

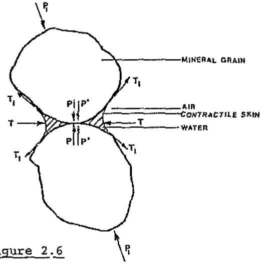

Figure 2.6

Consider two particles of soil in contact and acted upon by external forces P_1 (Figure 2.6). The forces P_1 need not be normal to the contact surfaces between the two particles and will consequently have two force components T and P which are tangent and normal to the contact surface respectively. Consider the angle between the force P_1 and the normal to the contact surface between the particles to be α (Figure 2.7).

Figure 2.7

It can then be said that,

$$
\left.\begin{aligned}
& T = P_1 \sin\alpha \\
\text{and} \quad & P = P_1 \cos\alpha \\
\text{and also,} \quad & \\
& T = P \tan\alpha
\end{aligned}\right\} \qquad \ldots(2.2)
$$

When α reaches its maximum value, ie just before the particles slip relative to each other, the value of $\tan\alpha_{max}$ is called the interparticle coefficient of friction μ,

$$\mu = \tan\alpha_{max} \qquad \ldots(2.3)$$

The maximum shear force T that can be sustained between the particles would thus be,

$$T = P\mu$$

From the above it can be concluded that slip failure will not occur if,

$$\frac{T}{P} \leq \mu \qquad \ldots(2.4)$$

Additional forces are caused by the menisci between the two particles which form at the contact point. The radius of a meniscus depends on the pressure difference between the air and the water phases and vice versa. The air is always at a higher pressure than the water and the resulting shape of the meniscus will be as shown in Figure 2.6. The higher the difference in air and water pressure the smaller will be the radius of the meniscus and the larger the tangential forces T_1. The force P' is the resultant effect of the tangential forces T_1 in the contractile skin and acts essentially normal to the contact surface. If one now makes the assumption that the

$$\left.\begin{aligned} T &= P_1 \sin \alpha \\ \text{and} \qquad P &= P_1 \cos \alpha \\ \text{and also,} \qquad & \\ T &= P \tan \alpha \end{aligned}\right\} \qquad \ldots(2.2)$$

When α reaches its maximum value, ie just before the particles slip relative to each other, the value of $\tan \alpha_{max}$ is called the interparticle coefficient of friction μ,

$$\mu = \tan \alpha_{max} \qquad \ldots(2.3)$$

The maximum shear force T that can be sustained between the particles would thus be,

$$T = P\mu$$

From the above it can be concluded that slip failure will not occur if,

$$\frac{T}{P} \leq \mu \qquad \ldots(2.4)$$

Additional forces are caused by the menisci between the two particles which form at the contact point. The radius of a meniscus depends on the pressure difference between the air and the water phases and vice versa. The air is always at a higher pressure than the water and the resulting shape of the meniscus will be as shown in Figure 2.6. The higher the difference in air and water pressure the smaller will be the radius of the meniscus and the larger the tangential forces T_1. The force P' is the resultant effect of the tangential forces T_1 in the contractile skin and acts essentially normal to the contact surface. If one now makes the assumption that the force P' does act normal to the contact surface it can be appreciated that this force does not have a shear component like the forces P_1.

By adding the force P' to P in equation (2.4) the ratio between the shear and normal forces will be decreased even more and (2.4) will become,

$$\frac{T}{(P+P')} \leq \mu \qquad \ldots(2.5)$$

The practical significance of this is that the stability of the two grains will increase. This increased stability between the grains will cause the soil structure to act more rigidly, leading to lower compressibility of unsaturated soils as compared to saturated soils. Blight (1965) actually showed experimentally that this is true by using a clayey loess type soil.

If the force P_1 is increased the value of the shear force T and the normal force P will both increase (equations (2.2)) which will lead to an increased value of the ratio in equation (2.5). The assumption is made that P' remains constant. If P_1 is increased continuously a stage will be reached where slip is imminent and then,

$$\frac{T}{(P+P')} \doteq \mu \qquad \ldots(2.6)$$

If the soil is now wetted so that the value of the tangential forces in the contractile skin (T_1) decrease with a subsequent decrease in the value of P', a stage will be reached where

$$\frac{T}{(P+P')} > \mu \qquad \ldots(2.7)$$

with failure occurring, leading to a sudden reduction in volume. This phenomenon does actually occur when collapsing sands which are subject to shearing stresses are wetted (see eg Blight, 1965 and Jennings and Burland, 1962).

If clay soils are dessicated considerably they disintegrate into clay *packets* which can easily be mistaken for individual grains when examining the soil (Burland, 1961 and Brackley, 1975).

The forces between the packets would be similar to those acting between the grains of a partly saturated granular soil.

When the soil is wetted two things happen. The frictional resistance between the particles may be exceeded with a subsequent decrease in the volume of the soil and secondly the clay packets take up water and swell (Brackley, 1975). The end result, ie whether the soil will increase or decrease in volume will depend on the magnitude of the applied load and on the properties of the soil. If the force developed in the clay due to swelling is greater than the applied load the soil will increase in volume and vice versa (Burland, 1965).

A partly saturated soil consisting of clay packets will be less rigid than an equivalent granular soil with the same pore water suction. The reason for this is that the individual packets are more plastic and will deform more readily under applied load than would solid soil particles. Blight (1965) compared compression curves for a partly saturated and saturated clay and from his results it can be seen that the slope of the two curves are very similar, indicating that the difference in compressibility is small.

volume. This phenomenon does actually occur when collapsing sands which are subject to shearing stresses are wetted (see eg Blight, 1965 and Jennings and Burland, 1962).

If clay soils are dessicated considerably they disintegrate into clay *packets* which can easily be mistaken for individual grains when examining the soil (Burland, 1961 and Brackley, 1975).

The forces between the packets would be similar to those acting between the grains of a partly saturated granular soil.

When the soil is wetted two things happen. The frictional resistance between the particles may be exceeded with a subsequent decrease in the volume of the soil and secondly the clay packets take up water and swell (Brackley, 1975). The end result, ie whether the soil will increase or decrease in volume will depend on the magnitude of the applied load and on the properties of the soil. If the force developed in the clay due to swelling is greater than the applied load the soil will increase in volume and vice versa (Burland, 1965).

A partly saturated soil consisting of clay packets will be less rigid than an equivalent granular soil with the same pore water suction. The reason for this is that the individual packets are more plastic and will deform more readily under applied load than would solid soil particles. Blight (1965) compared compression curves for a partly saturated and saturated clay and from his results it can be seen that the slope of the two curves are very similar, indicating that the difference in compressibility is small.

2.3 The Effective Stress Equation for Volume Change in Unsaturated Soil

It is not the intention to present and discuss all the proposed effective stress equations in literature. The Author is of the opinion that these have been well documented (eg Burland, 1961 and Fredlund and Morgenstern, 1977) and will only discuss the equation proposed by Bishop which seems to be widely accepted.

Bishop's effective stress equation is based on the assumption that the effective stress principle does apply to unsaturated soil and is given as,

$$\sigma' = \sigma - u_a + \chi(u_a - u_w) \qquad \ldots(2.8)$$

where σ' = effective stress

σ = total stress

u_a = pore-air pressure

u_w = porewater pressure

χ = effective stress parameter

The effectiveness parameter χ is a function of the degree of saturation of the soil, the soil structure, the cycle of wetting, drying and stress change leading to a particular degree of saturation and is also dependent on the value of $(u_a - u_w)$ (Bishop and Blight, 1963).

Bishop and Donald (1961) conducted an experimental study to prove the validity of equation (2.8) and found that if the value of the isotropic stress σ and the values of u_a and u_w in a triaxial test were changed in such a way that the values of $(\sigma - u_a)$ and $(u_a - u_w)$ remained constant, there was no change in the volume of the soil. If the values of σ, u_a and u_w were changed such that the values of $(\sigma - u_a)$ and $(u_a - u_w)$ varied, a change of volume resulted. From this study Bishop and Donald concluded that the form of equation (2.8) must be correct and that the behaviour of the soil was independent of the absolute values of u_a, u_w and σ.

Jennings and Burland (1962) expressed the opinion that the tests conducted by Bishop and Donald (1961) only proved that equation (2.8) is statically correct but did not demonstrate the validity of the principle of effective stress in unsaturated soil. They presented results of experiments which showed that certain soils behaved contrary to the predictions of the principle of effective stress. Soils investigated by Jennings and Burland suffered a reduction in volume when soaked under a constant load. This is contrary to equation (2.8) which indicates that as the value of $\chi(u_a-u_w)$ diminishes during wetting up, the effective stress actually decreases which should lead to an increase in volume.

Bishop and Blight (1963) discussed the volume change behaviour of unsaturated soils both at constant water content and when subjected to saturation. They concluded that the volume change behaviour of an unsaturated soil is highly dependent upon the stress path which it follows. This behaviour is best explained with the aid of Figure 2.8.

The behaviour of unsaturated soil is plotted in three-dimensional space with axes $(\sigma-u_a)$, (u_a-u_w) and void ratio e.

Consider point A. If the sample becomes saturated with $\sigma-u_a = 0$ it will increase in volume and swell to D. On the other hand, if it is soaked at constant volume an increase in stress $(\sigma-u_a)$ will be required for the sample to move to A'.

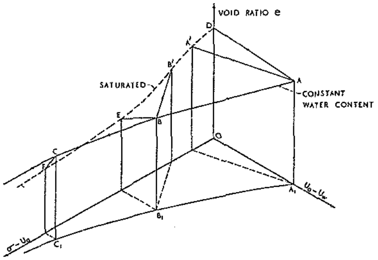

Figure 2.8 (After Bishop & Blight, 1963)

If the sample moves from B to B' when saturated (no volume change) a decrease in the value of $(\sigma-u_a)$ will be required and if it is saturated under constant load there will be a decrease in volume when it moves to E.

The position in three-dimensional space where the behaviour of the unsaturated soil sample changes from swelling to collapsing when saturated must be determined in the laboratory for each particular soil.

The object of this dissertation is to study the settlement of embankments constructed of *unsaturated, compacted soil* at a *constant moisture content* by using information obtained from oedometer tests. It is thus necessary to study the application of Figure 2.8 to this problem.

It will be noticed that changes in void ratio e and suction (u_a-u_w) of curve ABC (constant moisture content) in

Figure 2.8 are dependent on changes in the value of $(\sigma-u_a)$. An increase in $(\sigma-u_a)$ leads to decreases in both the void ratio and suction. It can thus be concluded that at constant water content $(\sigma-u_a)$ is the independent variable and (u_a-u_w) the dependent variable of the effective stress equation,

$$\sigma' = (\sigma-u_a) + \chi(u_a-u_w)$$

This conclusion is supported by experimental results obtained by Blight (1961). In these tests Blight first varied the values of σ, u_a and u_w in the triaxial cell in such a way that $(\sigma-u_a)$ and (u_a-u_w) remained constant within the soil specimen. Only the value of the isotropic stress σ was then increased. This change caused an increase in the value of u_w with the overall effect of an increase in $(\sigma-u_a)$ and a decrease in (u_a-u_w). Change in volume of the soil was measured throughout the whole test. Blight found that the change in volume for constant values of $(\sigma-u_a)$ and (u_a-u_w) was negligible while a sudden decrease in volume occurred when $(\sigma-u_a)$ was increased (see Figure 2.9).

The void ratio:effective stress curve obtained from an oedometer test on an unsaturated soil can be viewed as a projection of curve ABC on the void ratio: $(\sigma-u_a)$ plane in Figure 2.8. Changes in the suction (u_a-u_w) are thus indirectly taken into account by the shape of the void ratio:effective stress curve obtained from oedometer tests as changes in this parameter are dependent on changes in $(\sigma-u_a)$.

Blight (1961) also found that the flow of air through soil is similar to the flow of water through this medium but that the permeability of soil to air is higher. He presented consolidation:log time graphs from consolidation

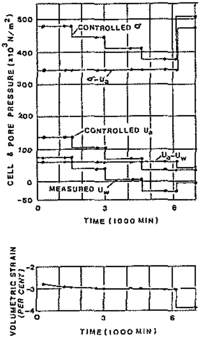

Figure 2.9 (After Blight, 1961)

tests on completely dry powdered kaolin which had a similar shape to the classical consolidation curve.

It should thus be possible to estimate settlements in embankments constructed of unsaturated soil by using soil properties obtained from oedometer tests on samples of the compacted unsaturated soil and by making use of the independent variables of the effective stress equation, viz σ' and $(\sigma-u_a)$ in an approximate form of the effective stress equation,

$$\sigma' = \sigma - u_a \qquad \ldots(2.9)$$

This equation would be valid for constant water content conditions until the soil becomes saturated by compression at which stage $u_a = u_w$, $(u_a-u_w) = 0$ and the equation becomes that for a saturated soil, viz,

$$\sigma' = \sigma - u_w \qquad \text{...(2.10)}$$

Until the soil becomes saturated by compression, only air will escape during the consolidation process. The pore-air pressure will always exceed the porewater pressure (see, eg Figure 3.1). As the pore-air pressure dissipates to atmospheric pressure, the porewater pressure in the vicinity of a drainage surface will always be below atmospheric pressure and, therefore, no porewater will drain from the soil unless the soil becomes saturated by compression.

It will thus be necessary to have a method to calculate excess pore-air pressures set up in the embankment during construction as well as a way to estimate dissipation of these excess pore-air pressures after completion.

The two conditions for this method to be successful are that the same stress path must be followed in the embankment and oedometer test and that the moisture content of the soil in the embankment remains unchanged.

Stress conditions in the oedometer and the embankments in terms of three-dimensional stress are of course not similar but are closely approximated in the centre core of the embankment which plays the major role in the settlement of the crest. The basic loading procedure in the sample and embankment is the same as both are first compacted and then subjected (at constant water content) to a continuous increase in loading until completion.

The moisture content in the main part of the embankment can be kept virtually constant even after the end of construction by installing filters in such a way as to intercept water seeping through the embankment during and after reservoir filling.

2.4 Conclusion

The fact that changes in effective stress (and thus volume changes) at constant water content are dependent on the value of $(\sigma - u_a)$ allows the use of soil properties obtained from oedometer tests in conjunction with the approximate effective stress equation,

$$\sigma' = \sigma - u_a$$

to estimate settlements of embankments. The shape of the oedometer curve indirectly takes account of the changes in suction $(u_a - u_w)$.

It is important that the stress path in the embankment be similar to that in the oedometer test and that the water content remains constant.

intercept water seeping through the embankment during and after reservoir filling.

2.4 Conclusion

The fact that changes in effective stress (and thus volume changes) at constant water content are dependent on the value of $(\sigma - u_a)$ allows the use of soil properties obtained from oedometer tests in conjunction with the approximate effective stress equation,

$$\sigma' = \sigma - u_a$$

to estimate settlements of embankments. The shape of the oedometer curve indirectly takes account of the changes in suction $(u_a - u_w)$.

It is important that the stress path in the embankment be similar to that in the oedometer test and that the water content remains constant.

CHAPTER 3

SETTLEMENT OF EMBANKMENTS CONSTRUCTED OF UNSATURATED COMPACTED SOILS

3.1 Introduction

In the previous chapter the consolidation of unsaturated soil was discussed qualitatively.

In this chapter a method will be developed with which settlement of embankment dams can be predicted by using standard laboratory equipment (the oedometer) and procedures to determine soil properties and then using these to estimate pore-pressures in embankments.

In the previous chapter it was concluded that a modified form of the effective stress equation can be used to estimate settlements at constant moisture content of embankments constructed of unsaturated soil. The approximate effective stress equation that will be used is given by,

$$\sigma' = \sigma - u_a \qquad \ldots (3.1)$$

where σ' = effective stress

σ = total stress

u_a = excess pore-air pressure

3.2 Estimating Pore-air Pressures in Unsaturated Soils

When a load is applied to a soil part of it is carried by the soil structure and part by the pore-fluid. An applied load would thus temporarily increase the pore-pressure. The amount with which the pore-pressure will increase will depend on the relative compressibilities of the pore-fluid and the soil structure. If the compressibility of the pore-fluid is much larger than that of the soil structure most the load increment

CHAPTER 3

SETTLEMENT OF EMBANKMENTS CONSTRUCTED OF UNSATURATED COMPACTED SOILS

3.1 Introduction

In the previous chapter the consolidation of unsaturated soil was discussed qualitatively.

In this chapter a method will be developed with which settlement of embankment dams can be predicted by using standard laboratory equipment (the oedometer) and procedures to determine soil properties and then using these to estimate pore-pressures in embankments.

In the previous chapter it was concluded that a modified form of the effective stress equation can be used to estimate settlements at constant moisture content of embankments constructed of unsaturated soil. The approximate effective stress equation that will be used is given by,

$$\sigma' = \sigma - u_a \qquad \ldots(3.1)$$

where σ' = effective stress

σ = total stress

u_a = excess pore-air pressure

3.2 Estimating Pore-air Pressures in Unsaturated Soils

When a load is applied to a soil part of it is carried by the soil structure and part by the pore-fluid. An applied load would thus temporarily increase the pore-pressure. The amount with which the pore-pressure will increase will depend on the relative compressibilities of the pore-fluid and the soil structure. If the compressibility of the pore-fluid is much larger than that of the soil structure most the load increment will be transferred directly to the soil structure and the increase in pore-pressure (the excess pore-pressure) will be relatively small.

The dissipation of the excess pore-pressure is responsible for the time-dependent volume change in soils and the degree of consolidation of an embankment is a measure of the dissipation of the excess pore-pressure.

One way of estimating the initial excess pore-pressure set up when load is applied to an unsaturated soil is to make use of the pore-pressure coefficients A and B proposed by Skempton (1954).

In defining the pore-pressure coefficient B Skempton first subjected a sample of soil in a triaxial apparatus to an increase in cell pressure $\Delta\sigma_3$ and measured the corresponding increase in pore-pressure Δu_1. B was then defined as,

$$B = \frac{\Delta u_1}{\Delta\sigma_3} \qquad \ldots(3.2)$$

Keeping the cell pressure constant and increasing the deviator stress by $(\Delta\sigma_1-\Delta\sigma_3)$ resulted in an increase of pore-pressure Δu_2 and Skempton showed that

$$\Delta u_2 = B.A(\Delta\sigma_1-\Delta\sigma_3) \qquad \ldots(3.3)$$

The total increase in pore-pressure is $\Delta u = \Delta u_1+\Delta u_2$ and by combining (3.2) and (3.3):

$$\Delta u = B\left(\Delta\sigma_3+A(\Delta\sigma_1-\Delta\sigma_3)\right) \qquad \ldots(3.4)$$

Bishop (1954) defined a pore-pressure coefficient $\bar{B}$ which he proposed to be used in the design of earth embankment dams,

$$\bar{B} = \frac{\Delta u}{\Delta\sigma_1} = B \,.\, \frac{1-(1-A)(1-K)}{1-B(1-A)(1-K)} \qquad \ldots(3.5)$$

where K = effective stress ratio = $\frac{\Delta\sigma_3'}{\Delta\sigma_1'}$

will be transferred directly to the soil structure and the increase in pore-pressure (the excess pore-pressure) will be relatively small.

The dissipation of the excess pore-pressure is responsible for the time-dependent volume change in soils and the degree of consolidation of an embankment is a measure of the dissipation of the excess pore-pressure.

One way of estimating the initial excess pore-pressure set up when load is applied to an unsaturated soil is to make use of the pore-pressure coefficients A and B proposed by Skempton (1954).

In defining the pore-pressure coefficient B Skempton first subjected a sample of soil in a triaxial apparatus to an increase in cell pressure $\Delta\sigma_3$ and measured the corresponding increase in pore-pressure Δu_1. B was then defined as,

$$B = \frac{\Delta u_1}{\Delta\sigma_3} \qquad \ldots(3.2)$$

Keeping the cell pressure constant and increasing the deviator stress by $(\Delta\sigma_1 - \Delta\sigma_3)$ resulted in an increase of pore-pressure Δu_2 and Skempton showed that

$$\Delta u_2 = B.A(\Delta\sigma_1 - \Delta\sigma_3) \qquad \ldots(3.3)$$

The total increase in pore-pressure is $\Delta u = \Delta u_1 + \Delta u_2$ and by combining (3.2) and (3.3):

$$\Delta u = B\left[\Delta\sigma_3 + A(\Delta\sigma_1 - \Delta\sigma_3)\right] \qquad \ldots(3.4)$$

Bishop (1954) defined a pore-pressure coefficient $\bar{B}$ which he proposed to be used in the design of earth embankment dams,

$$\bar{B} = \frac{\Delta u}{\Delta\sigma_1} = \frac{1-(1-A)(1-K)}{1-B(1-A)(1-K)} \qquad \ldots(3.5)$$

where K = effective stress ratio = $\frac{\Delta\sigma_3'}{\Delta\sigma_1'}$

The value of K for embankment dams will lie somewhere between the effective stress ratio K_o for soils at rest and K_f for soils where failure is imminent (Bishop, 1954).

The extreme values of $\bar{B}$ can be determined in the triaxial test by choosing appropriate values for K_o and K_f. The major principal stress σ_1 and the minor principal stress σ_3 are then changed simultaneously in the triaxial machine in such a way that

$$\Delta\sigma_1 = K_o.\Delta\sigma_3$$

or

$$\Delta\sigma_1 = K_f.\Delta\sigma_3$$

depending on the choice of effective stress ratio. By measuring the pore-pressure the value of $\bar{B}$ can be determined from:

$$\bar{B} = \frac{\Delta u}{\Delta\sigma_1}$$

(Bishop and Henkel, 1962).

By knowing the extreme values a reasonable estimate of $\bar{B}$ can be made to calculate pore-pressures in embankments.

The pore-pressure coefficients described above assume the existence of a single compressible fluid in the pore space and the effect of changes in suction are ignored.

Bishop and Henkel (1962) proposed pore-pressure coefficients for the air and water phases of an unsaturated soil,

$$\left.\begin{aligned} B_a &= \frac{\Delta u_a}{\Delta\sigma} \\ \text{and} \qquad B_w &= \frac{\Delta u_w}{\Delta\sigma} \end{aligned}\right\} \qquad \ldots(3.6)$$

Pore-air pressure is always higher than pore-water pressure in an unsaturated soil (Bishop and Henkel, 1962) and Blight (1961) found that the pore-air pressure set up in unsaturated soil during compaction could be above atmospheric pressure. Under increasing load the suction $(u_a - u_w)$ decreases and the pore-air and pore-water pressures converge (Figure 3.1).

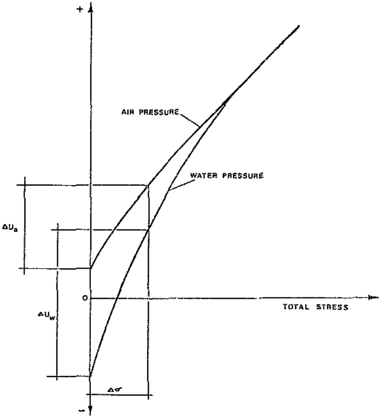

Figure 3.1

During this process the values of B_a and B_w both increase and tend towards one. At the point of convergence the soil becomes saturated and,

$$B_a = B_w = \bar{B} = 1 \quad \text{(neglecting the effect of shear)}$$

At this point all the excess pore-pressure is set up in the pore-water. This does not invalidate the assumption that effective stress in an unsaturated soil can be approximated by

$$\sigma' = \sigma - u_a$$

as u_a becomes u_w at the point of saturation.

In unsaturated soil the effective stress is dependent on $(\sigma - u_a)$ (see Chapter 2) and the pore-pressure coefficient of interest in this case is B_a.

To estimate values of B_a from oedometer test results it is necessary to know the change in pore-air pressure for a corresponding change in total stress. Conventional oedometers have no facility to measure pore-air pressure and a way must thus be found to estimate it.

Hilf (1948) and Bishop (1957) combined Boyle's and Henry's laws to estimate pore-air pressures in an unsaturated soil. The change in pore air pressure Δu_a corresponding to a change in volume ΔV is given by,

$$\Delta u_a = u_{ao} \cdot \frac{-\frac{\Delta V}{V_o}}{\frac{\Delta V}{V_o} + n_o(1-S_o+HS_o)} \qquad \ldots(3.7)$$

where u_{ao} = initial absolute air pressure in the pore space

V_o = initial total volume of soil

n_o = initial porosity of soil

S_o = initial degree of saturation

H = Henry's coefficient of solubility which is approximately 0,02 volumes of air per unit volume of water at normal temperatures.

It is important to note that a decrease in volume corresponds to a negative value for ΔV which will give a positive value for the pore-air pressure in equation (3.7).

Equation (3.7) is valid as long as there is air present in the sample of soil. As soon as the change in pore-air pressure exceeds,

$$\Delta u_a = u_{ao} \cdot \frac{(1-S_o)}{S_o H} \qquad \ldots(3.8)$$

the sample is saturated and an increase in pore pressure will be equal to the increase in total applied stress (ie $B_a \approx \bar{B} = 1$).

To estimate the value of B_a from oedometer tests it is necessary to know the relationship between $(\sigma-u_a)$ and volume change. This curve can be obtained by making the normal assumption that all the excess pore pressure in the oedometer has dissipated when the 24h volume change reading for a *specific* applied stress is taken. The total stress for an undrained condition can then be estimated by adding the excess pore-air pressure, as calculated from equation (3.7) for a specific value of $\frac{\Delta V}{V_o}$, to the corresponding value of $(\sigma-u_a)$, as indicated in Figure 3.2 .

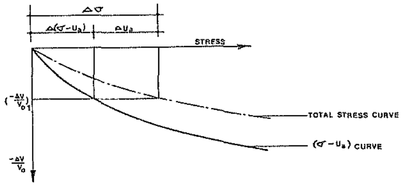

Figure 3.2

The value of B_a is given by,

$$B_a = \frac{\Delta u_a}{\Delta \sigma} \qquad \ldots(3.9)$$

To calculate the value of Δu_a in equation (3.7) the value of u_{ao} must be estimated. This value is usually assumed to be atmospheric pressure although there is evidence to show that this is not necessarily so in compacted soils (Blight, 1961). This should be kept in mind when estimating values of Δu_a and the sensitivity of B_a to various values of u_{ao} should be estimated. Increased values of u_{ao} will result in higher values for B_a.

3.3 Estimating End of Construction Pore-Air Pressures in Earth Embankments

Before discussing methods to estimate end of construction pore-air pressures in embankments, some of the factors affecting these pressures will be listed:

3.3.1 Construction rate

If the rate of construction of an embankment is high the end of construction pore-air pressures may be high. If the pore-air pressures are allowed to dissipate during construction by decreasing the construction rate these pressures would obviously be lower.

3.3.2 Properties of the soil

The properties of the soil which would most likely influence the end of construction pore-air pressures are the degree of saturation immediately after placing, permeability, compressibility and density.

(i) By increasing the degree of saturation in equation (3.7) the value of Δu_a will also be increased, leading to a higher value of B_a which in turn will be responsible for the development of higher pore-air pressures in the embankment.

(ii) The permeability of the soil will affect the amount of dissipation of excess pore-air pressure that will occur during the construction period. The higher the permeability the lower would be end of construction pore-air pressure.

(iii) The compressibility of the soil structure will control the fraction of total applied stress that will be transferred to the pore-air for a given degree of saturation. The higher the compressibility of the soil structure the higher will be the initial excess pore-air pressure.

(iv) The coefficient of consolidation c_v will be used as an alternative to the two properties mentioned above as it is a function of both the permeability and compressibility of the soil.

(v) The density of the soil determines the magnitude of the total stress increase with the addition of each layer during construction. The higher the density the higher will be the excess pore-air pressure (all other factors remaining constant.)

3.3.3 Geometry of Embankments

The geometry of the embankment will affect the dissipation process. If the embankment is low and extends for a considerable distance in the horizontal plane the dissipation of excess pore-air pressure would be essentially one-dimensional. On the other hand if the embankment has steep sides two-dimensional dissipation will occur (assuming that the embankment extends for a considerable distance in the third dimension and that dissipation in this direction is negligible.)

Hilf (1948) and Bishop (1957) proposed methods to estimate end of construction pore-air pressure in embankment dams. These methods were based on the following assumptions:

(i) No dissipation of excess pore-air pressure occurs during construction

(ii) The change in major principal stress ($\Delta\sigma_1$) could be approximated by the weight of a vertical column of soil directly above the point under consideration

(iii) The pore-pressure coefficient B_a is known or can be calculated.

In essence the pore-air pressure is estimated at a certain point by calculating the total stress caused by a column of soil directly above it and then this value is multiplied by the pore-pressure coefficient B_a to give the pore-air pressure. Figure 3.3 illustrates the above.

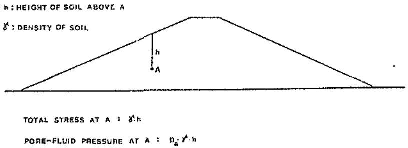

Figure 3.3

The effect of dissipation of pore-pressure during construction can also be studied in this way as was done by Bishop (1957) for the Usk dam. This dam was built in sections over three seasons with the bulk of the dissipation occurring at the end of each season. After a section had been completed a drainage blanket was laid before proceeding to construct the next section. It was found that the decreased compressibility of the soil due to dissipation and consolidation during the shutdown periods gave rise to lower values of the pore-pressure coefficient with a consequent lower rate of excess pore-pressure build-up during subsequent construction. The pore-pressure coefficient which was used to estimate the pore pressure in the second and third construction periods was obtained by allowing a certain percentage of dissipation in the undrained triaxial test before proceeding to simulate the loading for these periods.

The major principal stress σ_1 in an earth embankment is not vertical except on an axis of zero shear stress (Bishop, 1954). It is however reasonable to assume that σ_1 is vertical especially in the core under the crest of an embankment having an almost symmetrical cross-section.

Pore-air pressures at the end of construction, taking dissipation during the construction period into account can be estimated if it is assumed that although dissipation occurs in two dimensions, settlement occurs only in one. The theory developed here is an extension of the method used by Gibson (1958) to estimate pore-pressures in the Usk dam. All the assumptions normally made in settlement theory are also applicable here (see eg Terzaghi, 1943).

The equation governing two-dimensional dissipation of excess pore-air pressures is:

occurring at the end of each season. After a section had been completed a drainage blanket was laid before proceeding to construct the next section. It was found that the decreased compressibility of the soil due to dissipation and consolidation during the shutdown periods gave rise to lower values of the pore-pressure coefficient with a consequent lower rate of excess pore-pressure build-up during subsequent construction. The pore-pressure coefficient which was used to estimate the pore pressure in the second and third construction periods was obtained by allowing a certain percentage of dissipation in the undrained triaxial test before proceeding to simulate the loading for these periods.

The major principal stress σ_1 in an earth embankment is not vertical except on an axis of zero shear stress (Bishop, 1954). It is however reasonable to assume that σ_1 is vertical especially in the core under the crest of an embankment having an almost symmetrical cross-section.

Pore-air pressures at the end of construction, taking dissipation during the construction period into account can be estimated if it is assumed that although dissipation occurs in two dimensions, settlement occurs only in one. The theory developed here is an extension of the method used by Gibson (1958) to estimate pore-pressures in the Usk dam. All the assumptions normally made in settlement theory are also applicable here (see eg Terzaghi, 1943).

The equation governing two-dimensional dissipation of excess pore-air pressures is:

$$\frac{\partial u_a}{\partial t} = c_v \left(\frac{\partial^2 u_a}{\partial x^2} + \frac{\partial^2 u_a}{\partial y^2}\right) \qquad \ldots(3.10)$$

where u_a = *excess pore-air pressure*

t = time

c_v = coefficient of consolidation

x,y = coordinates of point under consideration

By applying the effective stress law it can be said for constant total stress that,

$$\frac{\partial u_a}{\partial t} = -\frac{\partial \sigma_y'}{\partial t} \qquad \ldots(3.11)$$

where σ_y' = *effective stress in y-direction (ie by* considering settlement in the y-direction only)

Equation (3.10) can be written as,

$$-\frac{\partial \sigma_y'}{\partial t} = c_v \left(\frac{\partial^2 u_a}{\partial x^2} + \frac{\partial^2 u_a}{\partial y^2}\right) \qquad \ldots(3.12)$$

The behaviour of an element in a *saturated* soil which increases in height with time will first be considered before proceeding to the behaviour of unsaturated soil.

Consider an element of soil at constant distance y from the base (Figure 3.4)

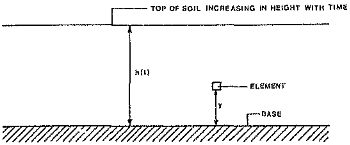

Figure 3.4

In Figure 3.4 h(t) is the height of the layer of soil expressed as a function of time.

The total stress in the y-direction at the element at any time can be written as,

$$\sigma_y = \gamma(h-y) \qquad \ldots(3.13)$$

where σ_y = total stress in y-direction

γ = density of the soil

By applying the effective stress principle,

$$\sigma_y = \sigma_y' + u = \gamma(h-y) \quad (u = \text{excess pore-water pressure})$$

or $$\sigma_y' = \gamma(h-y) - u \qquad \ldots(3.14)$$

Substituting equation (3.14) into (3.12) (for *saturated* soil),

$$\frac{\partial u}{\partial t} = c_v \left(\frac{\partial^2 u}{\partial x^2} + \frac{\partial^2 u}{\partial y^2}\right) + \gamma.\frac{\partial h}{\partial t} \qquad \ldots(3.15)$$

From equation (3.15) it can be concluded that the pore-pressure at any time is dependent on:

(i) The dissipation that has already occurred

$$\left[c_v \left(\frac{\partial^2 u}{\partial x^2} + \frac{\partial^2 u}{\partial y^2}\right)\right]$$

and (ii) The increase in pore-pressure caused by the increase in height of the embankment $(\gamma \frac{\partial h}{\partial t})$

If an *unsaturated* soil is used to construct an embankment, instead of a *saturated* soil, the increase in pore-pressure each time the embankment height is increased will be a fraction of that for a saturated soil due to the fact that the compressibility of the air is relatively higher than that of the soil structure.

The increase in pore-air pressure in an unsaturated soil can thus be written as $B_a . \gamma . \frac{\partial h}{\partial t}$. Equation (3.15) for an unsaturated soil can be rewritten as,

$$\frac{\partial u_a}{\partial t} = c_v \left(\frac{\partial^2 u_a}{\partial x^2} + \frac{\partial^2 u_a}{\partial y^2} \right) + B_a . \gamma . \frac{\partial h}{\partial t} \qquad \ldots (3.16)$$

3.4 The Coefficient of Consolidation c_v for Unsaturated Soil

So far all the constants required to calculate pore-pressure by using equation (3.16) are either known or can be estimated, except for the value of c_v. The determination of the coefficient of consolidation (c_v) for unsaturated soil from oedometer tests will now be dealt with.

To explain the determination of c_v for unsaturated soil, the typical curve for *saturated* soil will first be discussed. By plotting compression vs the square root of time for such compression to occur a typical curve as appears in Figure 3.5 usually results.

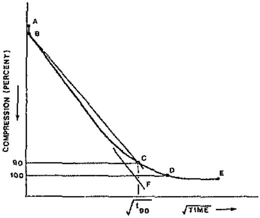

Figure 3.5

Three distinct stages can be identified from the curve:

(i) AB, the initial settlement which results mainly due to imperfections in the apparatus such as bedding down of the loading plate and possibly compression of small occluded bubbles of air in the saturated soil.

(ii) BD, the primary settlement which results from the slow transfer of load from the pore-water to the soil skeleton due to the dissipation of excess pore-water pressure during drainage.

(iii) DE, the secondary compression which occurs independently from any changes in effective stress and may be the result of changes in the electrical forces between the particles (see eg Burland, 1961).

A straight line (BF) drawn tangent to the primary consolidation curve intersects the ordinate axis at B. This point is called the corrected zero.

Figure 3.6 indicates the typical shape of a settlement curve for an *unsaturated* soil. It is similar to the curve for a saturated soil (Figure 3.5), except for a change in scale. The curve for an unsaturated soil can also be divided into three sections:

(i) AB, the initial settlement which is caused by the same factors as given for saturated soils with the additional effect of the larger difference between the compressibilities of the pore-fluid and the soil-structure. This component will be discussed in more detail further on.

(ii) BD, the primary settlement which results from the transfer of load from the pore-air to the soil-structure.

(iii) DE, the secondary compression

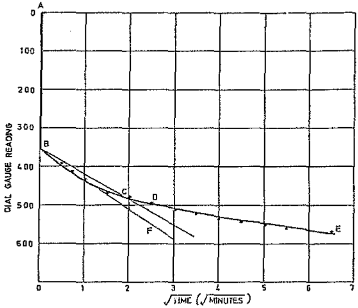

Figure 3.6

The *main reason for* the large difference between the initial settlements of the saturated and unsaturated soils can be attributed to the larger air content of the *unsaturated* soil.

Assume that the value of B_a is known for the soil being tested. If a load P is applied to the sample the excess pore-air pressure would increase by

$$\Delta u_a = B_a . P \qquad \ldots(3.17)$$

The *change in effective stress* in the soil at the instant of load application would be

$$\Delta\sigma' = P - B_a . P$$

or

$$\Delta\sigma' = (1 - B_a) . P \qquad \ldots(3.18)$$

This sudden increase in effective stress would result in an instantaneous settlement, presented by AB in Figure 3.6.

The root-time method used to calculate c_v for saturated soil is based on the *theoretical* shape of the settlement curve. The shape of the primary settlement part of the settlement curves in Figures 3.5 and 3.6 (sections BCD) are both determined by the dissipation of excess pore-pressure. The excess pore-pressure in an unsaturated soil is smaller than the excess pore-pressure in a saturated soil under similar load and the former also dissipates faster due to the higher permeability of the soil to air. The shape of the *primary* settlement curve for an unsaturated soil will however be similar to the classical theoretical shape of this part of the curve for a saturated soil (Blight, 1961).

It can thus be concluded that the excess pore-pressures in the two soils will dissipate in a similar way and the shape of the *theoretical* settlement curves for these parts of the actual settlement curves (sections BCD) would thus be similar. The position of 90% consolidation for unsaturated soil would thus be determined in exactly the same way as that for saturated soil by drawing line BC in Figure 3.6 in such a way that its abscissa is 1,15 times that of BF. The only difference in the determination of c_v for an unsaturated soil is that the distance AB (the initial settlement) is much larger. To predict the value of c_v for *unsaturated* soil as accurately as possible it is important to identify the corrected zero (that is the position of B) correctly. After the time for 90% consolidation is determined by drawing lines BF and BC from B the value of c_v can be estimated in the conventional way (see eg Taylor, 1948).

3.5 Settlement of Embankments Constructed of Unsaturated Soil

The ultimate settlement of the crest of an embankment can be given as,

$$\delta = \delta_i + \delta_c \qquad \ldots(3.19)$$

where δ_i = immediate settlement during construction

δ_c = consolidation settlement after completion.

The immediate settlement consists of three parts,

$$\delta_i = \delta_e + \delta_{inst} + \delta_{cons}$$

where δ_e = settlement of the crest caused by shear deformation in the embankment

δ_{inst} = instantaneous settlement due to the immediate increase in effective stress caused by the higher compressibility of the pore-air relative to the soil structure.

δ_{cons} = consolidation settlement that occurs during construction due to the dissipation of excess pore-air pressure during this period.

In this dissertation the *assumption* will be made that the effect of shear deformation on the settlement of the crest (δ_e) is negligibly small as compared to the instantaneous and consolidation settlement during construction. The equation for immediate settlement will thus be,

$$\delta_i = \delta_{inst} + \delta_{cons} \qquad \ldots(3.20)$$

To be able to estimate immediate settlement of an unsaturated soil a method is required to estimate the instantaneous increase in effective stress in the soil at load transfer as well as the dissipation of excess pore-air pressure during construction. This is provided by equation (3.16).

After completion of the embankment the term $B_a . \gamma . \frac{\partial h}{\partial t}$ in equation (3.16) falls away and settlement of the crest will be determined by,

$$\frac{\partial u_a}{\partial t} = c_v \left(\frac{\partial^2 u_a}{\partial x^2} + \frac{\partial^2 u_a}{\partial y^2} \right) \qquad \ldots (3.21)$$

The pore-air pressure in an embankment can thus be estimated at the end of construction by using equation (3.16) and with the aid of equation (3.21) the time-settlement curve can be estimated after completion.

To facilitate the calculation of settlement the central core can be divided into a number of horizontal layers as indicated in Figure 3.7

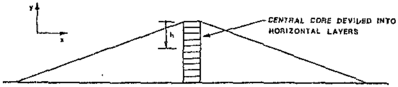

Figure 3.7

The average effective stress in each horizontal layer can be estimated by determining the average total stress and the average excess pore-air pressure for each horizontal layer.

The average total stress in each layer will be,

$$\sigma_y = \gamma . h \qquad \ldots (3.22)$$

where h = distance from the crest to the centre of the horizontal layer.

The average pore-air pressure $\bar{u}_a$ is the average value of the pore-air pressures at different positions in each layer as calculated with equations (3.16) and (3.21).

The average effective stress in each layer will thus be,

$$\sigma_y{}' = \sigma_y - \bar{u}_a \qquad \ldots(3.23)$$

The change in void ratio Δe can be determined for each layer from the e: log P curve for the soil used to construct the embankment (see Figure 3.8).

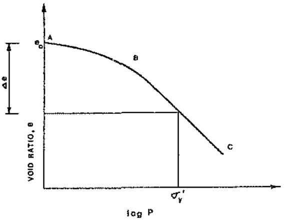

Figure 3.8

The total settlement at any time for any layer can be calculated as,

$$\delta_t = \frac{\Delta e}{1+e_o} \cdot H \qquad \ldots(3.24)$$

where e_o = initial void ratio

H = thickness of the layer of soil

The total settlement of the crest at any time is the sum of the settlements of the horizontal layers at the same time.

The immediate settlement δ_i is the settlement of the crest that has already occurred at the end of construction and the consolidation settlement δ_c is the difference between the ultimate settlement δ and the immediate settlement,

$$\delta_c = \delta - \delta_i \qquad \ldots(3.25)$$

The *ultimate* settlement (all excess pore-pressure has dissipated) can be calculated by using the e:log P curve and equating the effective stress to the total stress.

3.6 Conclusion

A method to estimate the pore-pressure coefficient B_a from oedometer test results has been presented.

The equation,

$$\frac{\partial u_a}{\partial t} = c_v \left(\frac{\partial^2 u_a}{\partial x^2} + \frac{\partial^2 u_a}{\partial y^2}\right) + B_a \cdot \gamma \cdot \frac{\partial h}{\partial t}$$

can be used to estimate pore-air pressures in embankments at the end of construction. This equation takes account of the factors affecting pore-air pressures in embankments at the end of construction which are construction rate, soil properties (c_v, B_a and γ) and embankment geometry.

Time-settlement curves for oedometer tests on unsaturated soil have larger initial settlements than similar curves for saturated soil. Care must be taken to correctly determine the position of the corrected zero before proceeding to estimate the value of c_v.

The ultimate settlement of an embankment consists of two components which are the immediate settlement δ_i which occurs during construction and the consolidation settlement δ_c which occurs after completion of the structure.

$$\delta = \delta_i + \delta_c$$

The settlement of the crest of an embankment can be calculated at any given time with the aid of the principle of effective stress and the relevant e:log P curve.

CHAPTER 4

DEVELOPMENT OF COMPUTER PROGRAM

4.1 Introduction

To apply the differential equation derived in the previous section in a computer program it must be written in finite difference form. This chapter will deal with the derivation of the finite difference equation and the basic philosophy of calculating pore-pressures in an earth embankment by using this equation. A flow chart of the developed program will also be presented. Only the calculation of pore-pressures in homogeneous embankments with filters will be considered.

4.2 Derivation of Finite Difference Equation

As mentioned in the previous chapter only dissipation of pore-air pressures in two dimensions will be taken into account. Consider part of a finite difference grid with equal grid dimensions in the horizontal and vertical directions as indicated in Figure 4.1

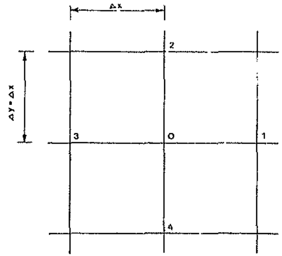

Figure 4.1

A finite difference equation will be derived to calculate the value of the pore-air pressure at node O one time step further. Equation (3.16) can be rewritten for convenience:

$$\frac{\partial u_a}{\partial t} = c_v \left(\frac{\partial^2 u_a}{\partial x^2} + \frac{\partial^2 u_a}{\partial y^2}\right) + B_a . \gamma . \frac{\partial h}{\partial t}$$

Let $\partial x = \Delta x$ = distance between the nodes

$\partial y = \Delta y$ = distance between the nodes

$\partial t = \Delta t$ = time step

$\partial h = \Delta h$ = increase in height per time step

$\frac{\partial^2 u_a}{\partial x^2}$ can be written in finite difference form as,

$$\frac{\partial^2 u_a}{\partial x^2} = \frac{u_3 - 2u_0 + u_1}{(\Delta x)^2}$$

and

$$\frac{\partial^2 u_a}{\partial y^2} = \frac{u_2 - 2u_0 + u_4}{(\Delta x)^2}$$

where u_0, u_1, ... etc are the pore-air pressures at the different nodes at a specified time.

Set the value of the pore-air pressure at node O one time step later = u_{ot}.

Equation (3.16) becomes,

$$\frac{u_{ot} - u_o}{\Delta t} = c_v \frac{1}{(\Delta x)^2} (u_1 + u_2 + u_3 + u_4 - 4u_0) + \gamma . B_a . \frac{\Delta h}{\Delta t}$$

or

$$u_{ot} = \frac{c_v . \Delta t}{(\Delta x)^2} (u_1 + u_2 + u_3 + u_4 - 4u_0) + u_0 + \gamma . B_a . \Delta h \qquad \ldots (4.1)$$

4.3 Calculation of Pore-Air Pressures

The calculation of pore-air pressure in an embankment under construction can be viewed as a calculation in three-dimensional space with axes x, y and t (Figure 4.2)

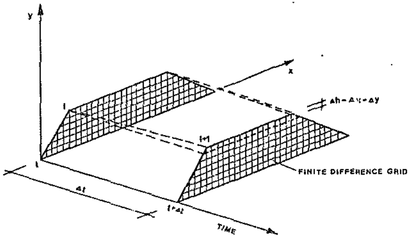

Figure 4.2

The most convenient way to calculate pore-air pressure which is set up during construction in the embankment is to let the increase in height for each time-step be equal to the vertical grid dimension (ie $\Delta h = \Delta y$). Figure 4.2 shows the change in embankment height for one small time-step Δt.

To calculate the pore-air pressures at each node on the finite difference grid at time $(t + \Delta t)$ by using equation (4.1) it is necessary to have a knowledge of the values of the pore-air pressures at each node at time-step t. It is thus necessary to initialise the values of the nodes in the first few layers when the calculation is commenced. If a fine grid is used inaccuracies in these initial values will not have a big influence on the ultimate values of the pore-air pressures at the end of construction. It is however desirable to have initial values that are as accurate as possible. To achieve this one could employ rigorous mathematical solutions of similar problems.

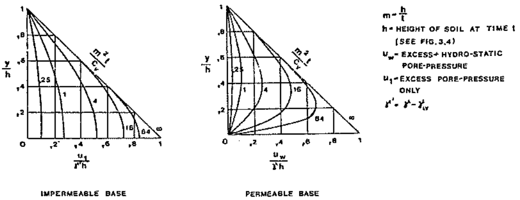

PORE PRESSURES IN A SATURATED CLAY LAYER INCREASING IN HEIGHT WITH TIME AT A CONSTANT RATE

(AFTER GIBSON, 1958)

Figure 4.3

Gibson (1958) published results of a rigorous mathematical solution of the differential equation for consolidation of a *saturated* layer of soil which increases in thickness with time at a constant rate. These solutions can be applied to layers of soil where the horizontal dimension is much larger than the vertical dimension and could thus be used to estimate pore-air pressures during the initial stages of construction of an earth embankment. These values must however be modified for *unsaturated* soil by multiplying them by B_a. To facilitate in estimating these pressures the results were presented in graphical form as indicated in Figure 4.3. A sample calculation demonstrating the use of these graphs is presented in Chapter 5.

To calculate the values of pore-air pressures at different time-intervals during construction there are basically two procedures to follow (also see Figure 4.4):

(i) In the centre part of the embankment load is added while dissipation occurs simultaneously and the complete equation must be used in this section (A), ie

$$u_{ot} = \frac{c_v.\Delta t}{(\Delta x)^2}\ (u_1+u_2+u_3+u_4-4u_0) + u_0 + B_a.\gamma.\Delta h$$

(ii) In the sections beneath the sloping sides (B) no additional load is added and only dissipation occurs, consequently only part of the finite difference equation must be used here,

$$u_{ot} = \frac{c_v.\Delta t}{(\Delta x)^2}\ (u_1+u_2+u_3+u_4-4u_0) + u_0 \qquad ...(4.2)$$

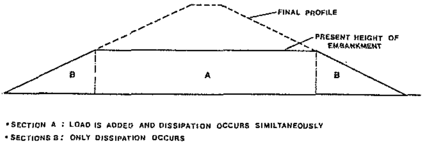

Figure 4.4

It is common practice to install pressure relief filters in embankments when high pore-pressures are expected. The pore-pressures at these filters remain zero at all times with a resultant effect on the pore-air pressures at the nodes on the finite difference grid surrounding them. The filter nodes should be identified in the finite difference program and kept at zero pore-air pressure at all times.

In the program developed in this dissertation the base of the embankment is assumed to be horizontal. Two drainage conditions are possible at the base which can be either permeable or impermeable.

If the base is permeable the excess pore-air pressures at the base will be zero at all times. These nodes can thus be treated as if they were filters.

Estimating pore-air pressures on an impermeable base presents a problem. Figure 4.5 indicates the nodes that should be considered when calculating pore-air pressures at node O on an impermeable base.

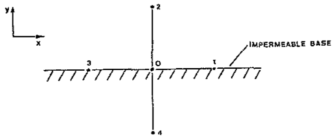

Figure 4.5

All the pore-air pressures required to calculate u_{ot} from equation (4.1) or (4.2) are known except the pressure at node 4. By making the assumption that the pressure difference between nodes 1 and 3 is negligible, which is a reasonable assumption when a fine finite difference grid is used, it can be said that,

$$\frac{\partial u}{\partial y} = 0 \qquad \ldots(4$$

at the impermeable boundary.

Write equation (4.3) in finite difference form,

$$\frac{u_2 - u_4}{2\Delta y} = 0$$

or $$u_2 = u_4 \qquad \ldots(4.4)$$

All the values of the nodes within the impermeable base (the so-called *ghost* nodes) can thus be set equal to the values of the nodes on the opposite side of the base boundary and the value of u_{ot} calculated by using either equation (4.1) or (4.2) depending on circumstances.

The pore-air pressures at the free boundaries of the earth embankment will remain zero at all times and need not be recalculated.

The recalculation of pore-air pressures during construction in the row of nodes just below the moving top boundary of the embankment also require special consideration. If the finite difference equation is considered for the nodes in the top row, ie the moving boundary, at time t just before the new load is added then,

$$\gamma . B_a . \Delta h = 0$$

and $$u_{ot} = 0$$

The finite difference equation then becomes,

$$\frac{c_v . \Delta t}{(\Delta x)^2} (u_1 + u_2 + u_3 + u_4 - 4u_0) + u_0 = 0 \qquad \ldots(4.5)$$

Nodes 0, 1 and 3 are on the top boundary and the value of pore-air pressure at these nodes is zero. Equation (4.5) thus becomes,

$$u_2 = -u_4 \qquad \ldots(4.6)$$

The value of the *ghost* node (node 2) is thus known.

The pore-air pressure at node 0 at time t + Δt can be calculated as,

$$u_{ot} = \frac{c_v.\Delta t}{(\Delta x)^2}(u_1 - u_4 + u_3 + u_4 - 4u_0) + u_0 + B_a.\gamma.\Delta h$$

$$= B_a.\gamma.\Delta h \qquad (u_1 = u_3 = u_0 = 0)$$

It can thus be concluded that the values of pore-air pressure at the nodes in the row just below the top moving boundary at time t + Δt are given by

$$u_{ot} = B_a.\gamma.\Delta h \qquad \ldots(4.7)$$

4.4 Flow Chart for Computer Program

Before presenting the flow chart, the basic calculating procedure will be discussed. The embankment to be analysed must first be placed into a coordinate system (or *finite difference grid*). The coordinate system that was chosen to be used in this program consists of horizontal rows with a numbering system that changes a thousand at a time. The vertical columns were numbered in normal sequence (see Figure 4.6). *In a system* like this each node has a specific number, eg the number of node A in Figure 4.6 is 3003.

The procedure followed in the computer program was to recalculate the pore-air pressure at each node for a new time-step in a *row by row sequence*. By following a sequence like this it is only necessary to have a knowledge of the first and last node numbers in each row as well as the number of the last row to define the geometry of the embankment.

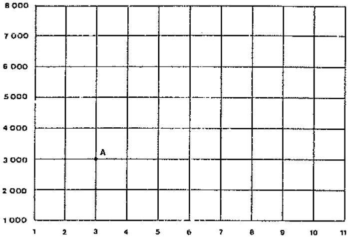

Figure 4.6

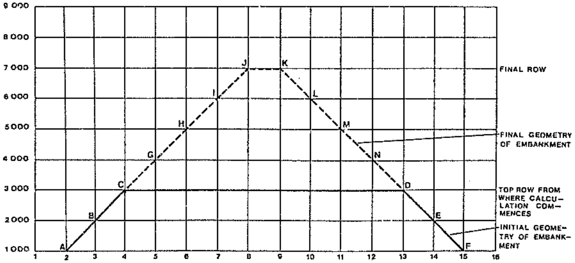

Figure 4.7

To be able to commence the calculation initial values of pore-air pressures in the first few constructed rows must also be known. These values are obtained by making use of Figure 4.3. The row number of the top row where analysis commences must be known. See Figure 4.7 for clarity.

It should be noted here that if row numbers are used to define geometry, the actual number of the row is used, ie 1 instead of 1 000, 2 instead of 2 000 etc. The numbering system proposed in Figure 4.6 refers only to the numbers of the nodes.

Referring to Figure 4.7 the initial data required to define the initial and final geometry of the embankment would be:

Number of final row (N): 7

Number of row from where calculation commences (IS): 3

Node numbers to define free boundary of embankment:

Row	First Node	Last Node
1	1002	1015
2	2003	2014
3	3004	3013
4	4005	4012
5	5006	5011
6	6007	6010
7	7008	7009

The initial values of pore-air pressures for nodes

1001 through 1015
2001 through 2015
3001 through 3015

are also required. (Note that the initial pore-pressure value of node 2002 for example will be zero).

The calculation is now continued by calculating new values for pore-air pressures at each node after an additional layer has been added.

When row 7 has been reached the pore-air pressures can be calculated for an undetermined time by allowing dissipation of pore-air pressures only. This calculation enables one to predict a settlement curve for the embankment.

Two arrays are used in the calculation of pore-pressures. Array P is used for the pore-pressure values in time-step t and array B for those in time-step $(t + \Delta t)$. After all the pore-pressures in a new time-step have been recalculated the values of array B are placed into array P and the procedure repeated.

The following flow chart symbols will be used.

FLOW CHART SYMBOL	COMMENTS
	READING OF DATA
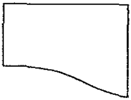	WRITE
	EXECUTABLE STATEMENT
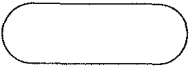	DECISION STATEMENT

FLOW CHART FOR CALCULATING PORE-AIR PRESSURES

IN AN EARTH EMBANKMENT

Flow Chart

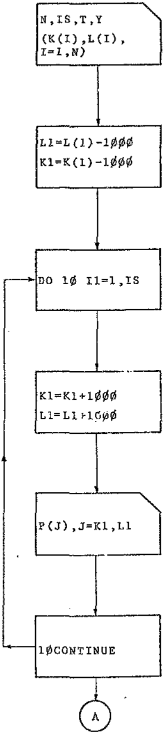

Comments

N = Total number of rows

IS = Number of top row when calc commences

T = time-step

Y = grid dimension

K(I),L(I) = first and last nodes of each row

Read in values of initial pore-pressures in first few layers (ie 1 to IS) in a row by row sequence

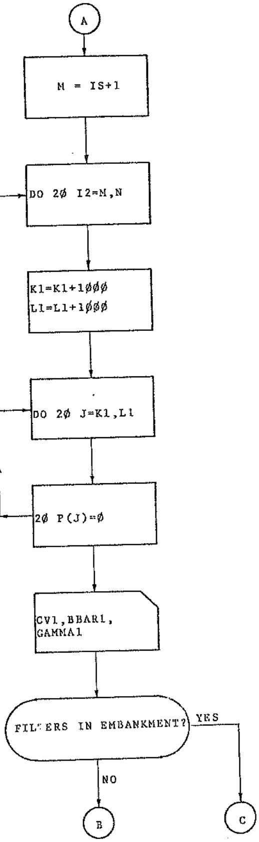

Initialize all the pore-pressure values of the non-constructed nodes

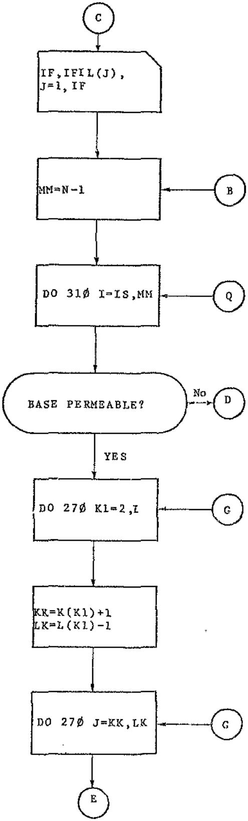

IF=Number of filters in embankment

IFIL(J)=Node numbers of filters

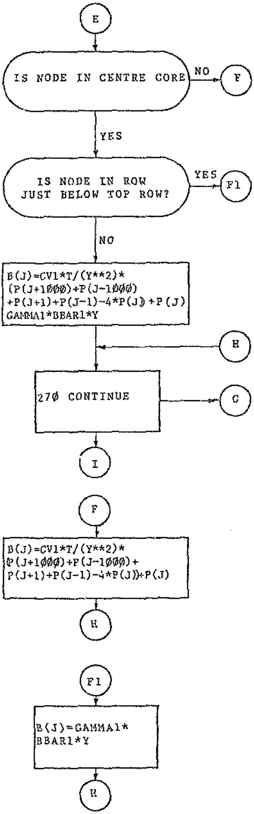

Recalculate pore-pressures in permeable based embankment (central core)

Recalculate pore-pressures in sides

Recalculate pore-pressures in row just below top row

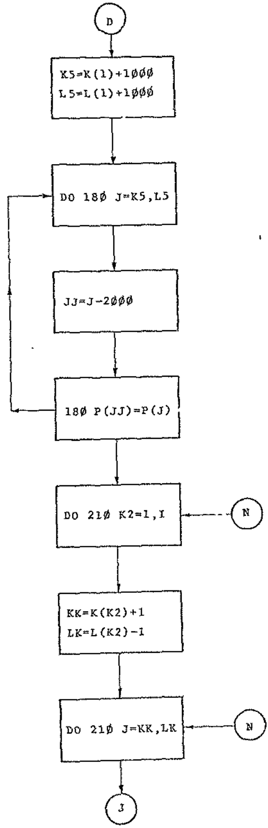

Give values to *Ghost* nodes in impermeable base

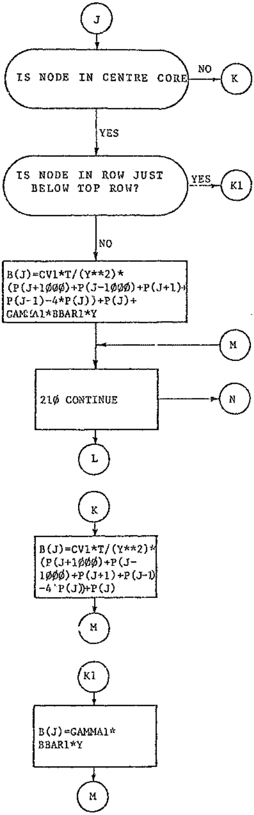

Recalculate pore-pressures in impermeable based embankment (central core)

Recalculate pore-pressures in sides

Recalculate pore-pressures in row just below top row

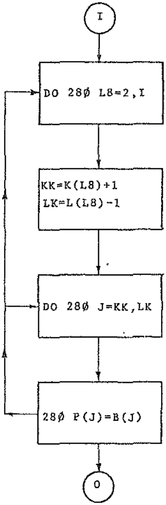

Place recalculated pore-pressures from array B into array P for permeable base

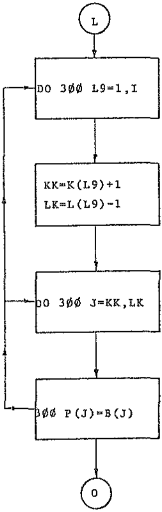

Place recalculated pore-pressures from array B into array P for impermeable base

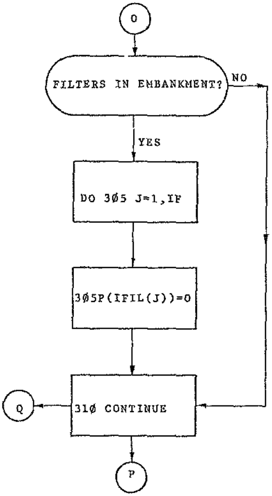

Set the pore-
pressures at all
filters = Ø

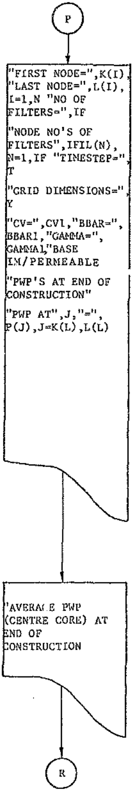

Print all relevant data and pore-pressures at each node at end of construction

Print heading for values of average pore-pressures in centre core which will be used to calculate settlement

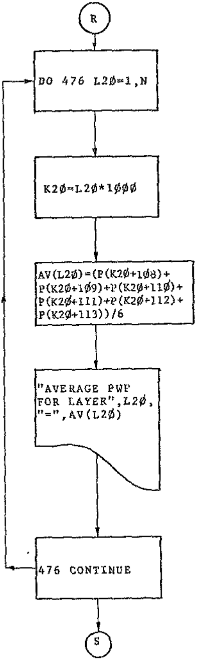

Calculate average
pore-pressures in
centre core at end
of construction

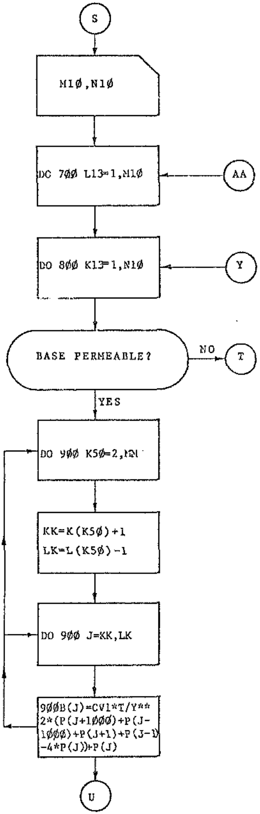

Calculation of pore-pressures at different intervals after construction commences here.

M1Ø=Number of intervals where pore-pressures is required

N1Ø = Number of time-steps per interval

Recalculate pore-pressures at different time-intervals for permeable base after completion of embankment

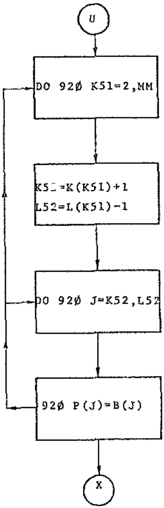

Place recalculated
pore-pressures into
array P from array B

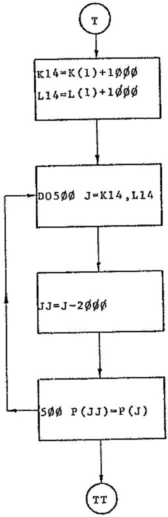

Give values to *ghost* nodes in impermeable base

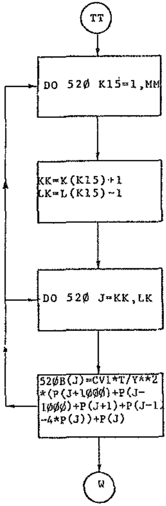

Recalculate
pore-pressures at
a new time-step
for impermeable base
after construction
is complete

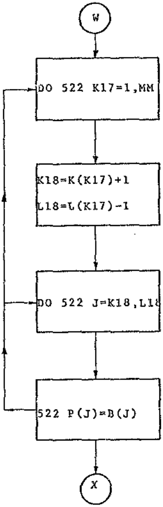

Place recalculated pore-pressures into P array from B array

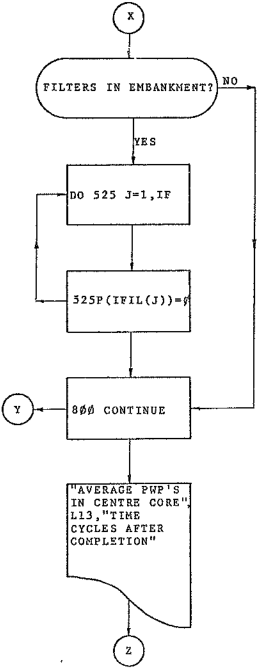

Set pore-pressures at filters =Ø

Print heading for values of average pore-pressures in centre core at a certain interval after completion

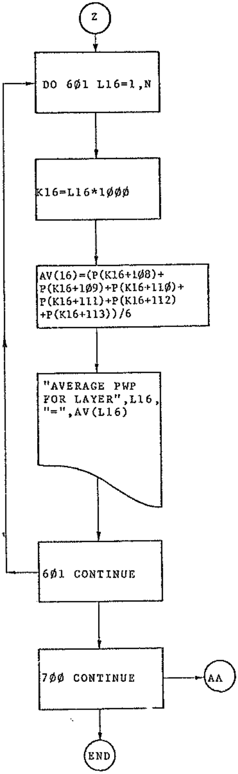

Calculate average pore-pressures in central core row by row and print results

CHAPTER 5

RESULTS

5.1 Introduction

In this chapter the results are given of settlement calculations performed for the Mita Hills dam in Zambia. The calculated settlements are compared with the measured settlements.

5.2 Description of Embankment Dam

The Mita Hills dam that was used as a case study in this dissertation is located near Kabwe in Zambia and was built in 1957 to provide augmented hydro-electric power for the Broken Hill mine.

The Mita Hills embankment has a maximum height of 48,8 m and a crest length of 366 m. It was built of rolled earthfill and has a sloping filter as well as twelve pore-pressure relief drains in the downstream zone. A schematic plan of the dam and a section at maximum height are given in Figures 5.1 and 5.2.

The sub-tropical climate of Zambia forced construction of the whole dam to be completed within the dry season which is between July and December. To place the fill of approximately one and a quarter million cubic metres in six months required working 22 hours a day for seven days a week.

The high construction rate required sophisticated quality control techniques as there was no time to do any substandard work. The techniques which were used to control quality were described by Blight (1962).

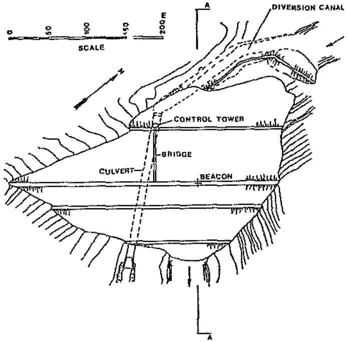

PLAN OF DAM

(AFTER LEGGE, 1970)

FIGURE 5.1

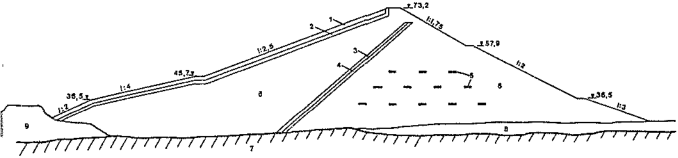

0 10 20 30 50 100m

SCALE

1. 1,5m ROCKFILL
2. 1,2m NATURAL GRAVEL
3. 0,9m NATURAL GRAVEL
4. 0,9m COARSE FILTER MATERIAL
5. PORE-PRESSURE RELIEF DRAINS
6. UNIFORM ROLLED FILL
7. ROCK
8. RIVER SAND
9. BANK OF DIVERSION CANAL

MAX. HEIGHT: 48,8m

SECTION AA OF EMBANKMENT

FIGURE 5,2

5.3 Finite Difference Grid and Constants

5.3.1 Finite difference grid

For the purpose of calculating pore-pressures and settlements in the embankment the assumption was made that the embankment base was horizontal and straight. This assumption is reasonable except at the toe on the upstream side of the embankment. A fine finite difference grid with dimensions of 1,28 m x 1,28 m was used as a coordinate system as indicated in Figure 5.3

The number system is the same as explained in Chapter 4.

5.3.2 Sensitivity of constants

By inspecting the finite difference equation,

$$u_{ot} = \frac{c_v.\Delta t}{(\Delta x)^2} . (u_1+u_2+u_3+u_4-4u_0) + u_0 + \gamma.B_a.\Delta h$$

four variable constants for a specified finite difference grid can be identified,

c_v = coefficient of consolidation

Δt = time-step

γ = density of the soil

B_a = pore-pressure coefficient

A sensitivity analysis was carried out to determine the influence of these constants on the excess pore-air pressures in the embankment at the end of construction. This analysis was done by changing the values of the constants in the finite difference computer program one at a time. The average pore-air pressure at the end of construction of all the nodes in column 111 (Figure 5.3) was calculated in each case and plotted against the values of the corresponding constants in Figure 5.4.

It was decided to determine the change in average pore-air pressure in column 111 for ±10 per cent changes in the various

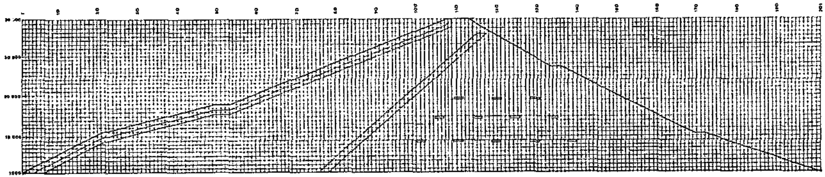

FIGURE 5.3

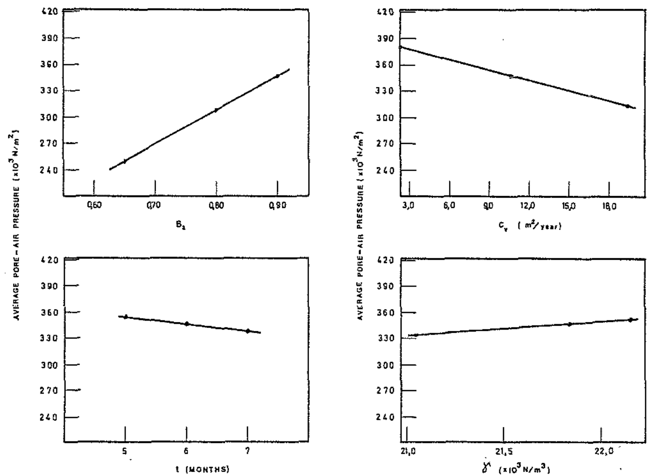

SENSITIVITY OF PORE-AIR PRESSURE TO CHANGES IN CONSTANTS

FIGURE 5.4

constants to have a common basis to compare their relative importance (Figure 5.5).

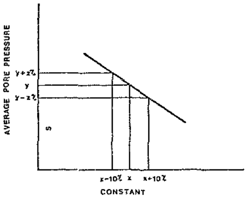

Figure 5.5

The results of this investigation are given in Table 5.1:

TABLE 5.1

Percentage Changes in Average Pore-Air Pressures for ± 10 per cent Changes in Values of Constants

Constant	Percentage Change in Pore-Air Pressure
B_a	± 10,0
C_v	∓ 1,2
t	∓ 1,3
γ	± 10,0

From Table 5.1 it can be concluded that the pore-air pressure at the end of construction is very sensitive to changes in the values of B_a and γ, and relatively insensitive to changes in c_v and t.

5.3.3 Choice of constants

5.3.3.1 Density of soil γ

Considering the fact that excess pore-air pressures at the end of construction are very sensitive to changes in the density of the soil it was decided to vary the density in the settlement calculations. Average and extreme values of density were estimated.

Density of the soil was calculated by using the following equation,

$$\gamma = \frac{G_s(1+w)}{1+e} \cdot \gamma_w \qquad \ldots(5.1)$$

where G_s = specific gravity of mineral grains
w = moisture content
e = void ratio
γ_w = density of water = 10^4 N/m^3

The values of these constants were obtained from the laboratory report on the soil which was used to construct the embankment and were,

G_s = 2,60
w = 0,1143

Two values for the void ratio e had to be assumed. The average value of e was assumed to be approximately half way between the maximum and minimum void ratios on the e:log P curve (see Figure 5.9) and was,

$$e = 0{,}314$$

The extreme value of e was taken as,

$$e = 0{,}280$$

The densities calculated were,

average $\gamma = 22{,}1 \times 10^3\ N/m^3$

extreme $\gamma = 22{,}6 \times 10^3\ N/m^3$

5.3.3.2 Coefficient of consolidation

Table 5.1 indicates that the pore-air pressure is not very sensitive to changes in c_v and it was consequently decided to use only one value of c_v in all the settlement calculations.

The value of c_v for unsaturated soil was calculated from oedometer test results by using the method described in Chapter 3. It was found that the value of c_v decreased as the applied pressure in the oedometer increased (Figure 5.6). The value of c_v used in the settlement calculations was taken as the average of all these values,

$$c_v = 10{,}5\ m^2/year$$

5.3.3.3 Pore-pressure coefficient B_a

The pore-air pressures in the embankment at the end of construction are sensitive to changes in B_a and it was consequently decided to vary the value of B_a for different settlement calculations.

The values of B_a were calculated with the equations given in Chapter 3,

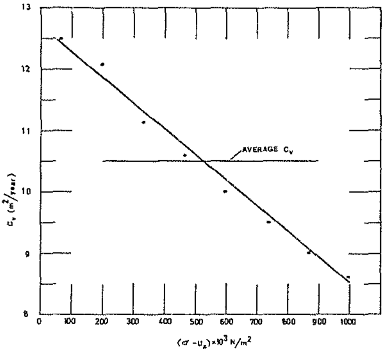

Figure 5.6

$$\Delta u_a = u_{ao} \cdot \frac{-\frac{\Delta V}{V_o}}{\frac{\Delta V}{V_o} + n_o(1-S_o+S_o.H)}$$

and $$B_a = \frac{\Delta u_a}{\Delta \sigma}$$

The different values of B_a were estimated by firstly varying the value of the initial pore-air pressure (u_{ao}) and secondly by making two different assumptions in calculating the constant average values of B_a which were used throughout the embankment in the different settlement calculations.

The values for u_{ao} that were used were atmospheric pressure (100×10^3N/m^2 absolute) and a higher pressure which was assumed as 150×10^3 N/m^2 (absolute). The assumption that u_{ao} is atmospheric is normally used in calculations of this kind

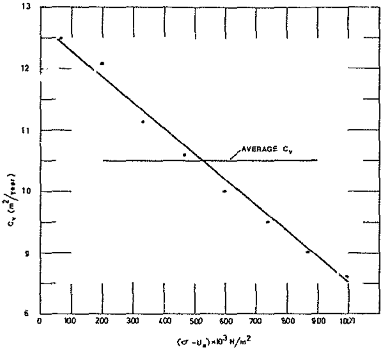

Figure 5.6

$$\Delta u_a = u_{ao} \cdot \frac{-\frac{\Delta V}{V_o}}{\frac{\Delta V}{V_o} + n_o(1 - S_o + S_o . H)}$$

and $$B_a = \frac{\Delta u_a}{\Delta \sigma}$$

The different values of B_a were estimated by firstly varying the value of the initial pore-air pressure (u_{ao}) and secondly by making two different assumptions in calculating the constant average values of B_a which were used throughout the embankment in the different settlement calculations.

The values for u_{ao} that were used were atmospheric pressure (100 x $10^3 N/m^2$ absolute) and a higher pressure which was assumed as 150 x 10^3 N/m^2 (absolute). The assumption that u_{ao} is atmospheric is normally used in calculations of this kind

(Hilf, 1948 and Bishop, 1957). The assumption of the higher value of u_{ao} was based on measurements of pore-air pressure in compacted Mangla shale (Blight, 1961). The initial absolute pore-air pressure values were thus assumed to be

$$u_{ao} = 100 \times 10^3 \ N/m^2$$

and $$u_{ao} = 150 \times 10^3 \ N/m^2$$

Results of the calculations of values of B_a are given in Tables 5.2 and 5.3.

TABLE 5.2

Values of B_a Calculated from Oedometer Results
$u_{ao} = 100 \times 10^3 \ N/m^2$

$-\frac{\Delta V}{V_o}$	$\Delta(\sigma - u_a)$ ($\times 10^3$ N/m^2)	Δu_a ($\times 10^3$ N/m^2)	$\Delta\sigma$ ($\times 10^3$ N/m^2)	$B_a = \frac{\Delta u_a}{\Delta\sigma}$	Average B_a
0,0117	35,2	42,4	77,6	0,55	0,60
0,0197	70,3	98,5	168,8	0,58	
0,0297	140,6	230,5	371,1	0,62	
0,0335	225,0	502,4	727,4	0,69	
0,0361	281,2	*	*	1,0	1,00

*The sample had become saturated and the equation for Δu_a was no longer valid

A comparison of Tables 5.2 and 5.3 shows that higher initial pore-air pressure in compacted soil leads to higher values of B_a.

TABLE 5.3

Values of B_a Calculated from Oedometer Results

$u_{ao} = 150 \times 10^3\ N/m^2$

$\frac{\Delta V}{V_o}$	$\Delta(\sigma - u_a)$ $(x10^3\ N/m^2)$	Δu_a $(x10^3\ N/m^2)$	$\Delta\sigma$ $(x10^3\ N/m^2)$	$B_a = \frac{\Delta u_a}{\Delta \sigma}$	Average B_a
0,0117	35,2	65,9	101,1	0,65	0,73
0,0197	70,3	158,7	229,0	0,69	
0,0279	140,6	401,5	542,1	0,74	
0,0335	225,0	1041,7	1266,7	0,82	
0,0383	337,0	*	*	1,00	1,00

In order to use the assumption that the values of the constants c_v, B_a and γ throughout the embankment are fixed a method must be found to estimate a weighted average value for B_a. Two methods were employed in this dissertation. The first method is based on the assumption that the average value of B_a is weighted proportionally to the cross-sectional areas occupied by the different B_a values.

The second method is based on the assumption that B_a is weighted proportionally to the height occupied by each B_a value in a ver'ical column of soil in the central core.

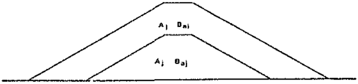

$$B_a = \frac{A_i}{A} B_{ai} + \frac{A_j}{A} B_{aj}$$

$$A = A_i + A_j$$

METHOD 1

Figure 5.7

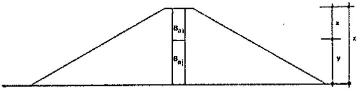

$B_a = \frac{x}{z} B_{ai} + \frac{y}{z} B_{aj}$

METHOD 2

Figure 5.8

Settlements calculated by using the B_a values obtained from the two methods could be compared with the measured settlements to determine which method is better.

The following average B_a values were estimated:

$\underline{B_a \text{ values for } u_{ao} = 100 \times 10^3 \ N/m^2}$

Weighted area method:

B_a = 0,90 x 0,60 + 0,10 x 1,00 = 0,64
say 0,65

Weighted column method:

B_a = 0,64 x 0,60 + 0,36 x 1,00 = 0,74
say 0,75

$\underline{B_a \text{ values for } u_{ao} = 150 \times 10^3 \ N/m^2}$

Weighted area method:

B_a = 0,93 x 0,73 + 0,07 x 1,00 = 0,75

Weighted column method:

$$B_a = 0,69 \times 0,73 + 0,31 \times 1,00 = 0,81$$

say 0,80

An extreme value calculation was also performed with an average value of B_a that would most probably never have occurred.

$$B_a = 0,90$$

5.3.3.4 Construction time t

The assumption was made that the rate of construction was linear. If the schematic plan of the dam in Figure 5.1 is inspected it can be seen that this assumption should be reasonable. Even if there were small deviations from the assumed rate of construction the difference between actual and estimated pore-air pressures at the end of construction due to this variable should be negligibly small as can be seen in Table 5.1.

The embankment was constructed over a period of six months and the time-step required to construct one layer in the finite difference grid is thus,

$$\Delta t = \frac{0,5 \text{ year}}{38 \text{ layers}} = 0,013 \text{ year/layer } (4,7 \text{ days/layer})$$

5.3.3.5 Summary of constants

Table 5.4 presents a summary of the constants used to calculate the average and extreme settlements.

TABLE 5.4

Summary of Constants

Constant	Average Values			Extreme Values
B_a	0,65	0,75	0,80	0,90
γ (x10³ N/m³)	22,1	22,1	22,1	22,6
Δt (year/layer)	0,013	0,013	0,013	0,013
c_v (m²/year)	10,5	10,5	10,5	10,5

5.3.4 Initial Pore-air pressures

As mentioned previously values of initial pore-air pressures are required to commence the finite difference calculation of pore-air pressure in the embankment. It is necessary to estimate values for the first few constructed layers by means of the graphs presented by Gibson (1958). These graphs are in terms of dimensionless parameters (Figure 4.3),

$\frac{y}{h}$ and $\frac{u_1}{\gamma' h}$ - impermeable base

and $\frac{y}{h}$ and $\frac{u_w}{\gamma h}$ - permeable base

where $\gamma' = \gamma - \gamma_w$ ...(5.2)

To estimate pore-pressures in saturated soils a constant c is determined from these graphs and the pore-pressures at different positions calculated as,

$u = c.\ \gamma'.h + \gamma_w.h$ - impermeable base

and $u = c.\gamma.h$ - permeable base

In unsaturated soil the pore-air pressure is only a fraction of the pore-pressure in saturated soil and by applying the pore-pressure coefficient B_a the pore-air pressure in an unsaturated soil can be estimated as,

$$\left.\begin{aligned} u_a &= B_a(c.\gamma'.h+\gamma_w.h) && \text{- impermeable base} \\ \text{and} \quad u_a &= B_a.c.\gamma.h && \text{- permeable base} \end{aligned}\right\} \quad \ldots(5.3)$$

It must be kept in mind that the graphs presented by Gibson (1958) take account of one-dimensional dissipation of pore-pressure only. It is however reasonable to assume that this condition exists in the initial stages of construction when the vertical dimension of the soil layer is small compared to the horizontal dimension. Even if these estimated pore-air pressures are not absolutely correct the error will be partially phased out each time the finite difference calculation is repeated and the effect on the final value of pore-air pressure at the end of construction should be negligible.

In calculating pore-air pressures for the Mita Hills embankment dam the assumption was made that five layers (6,40 m) had already been constructed when the finite difference calculation commenced.

As can be seen in Figure 5.2 one section of the dam is built on an impermeable base and another section on river sand which is deemed permeable. It was thus necessary to estimate two sets of initial pore-air pressures by using Gibson's (1958) graphs and equations (5.3). The values of pore-pressures are presented in Tables 5.5 and 5.6. Note that the values in these tables are pore-pressures for a saturated soil which were corrected in the computer program by adding a DO-loop which multiplied them by the appropriate B_a value.

TABLE 5.5

Pore-Pressures for a Permeable Base

($x10^3$ N/m^2)

Position	Pore-Pressure	
	Average	Extreme
0	0	0
1	28,3	28,9
2	56,6	57,9
3	77,8	79,6
4	87,7	89,7
5	0	0

$(\frac{m^2t}{c_v} = 60)$

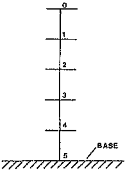

TABLE 5.6

Pore-Pressures for an Impermeable Base

($x10^3$ N/m^2)

Position	Excess Pressure		Hydrostatic Pressure	Total Pressure	
	Average	Extreme		Average	Extreme
0	0	0	0	0	0
1	15,5	16,1	12,8	28,3	28,9
2	31,0	32,3	25,6	56,6	57,9
3	46,5	48,4	38,4	84,9	86,8
4	60,4	62,9	51,2	111,6	114,1
5	63,5	66,1	64,0	127,5	130,1

$(\frac{m^2t}{c_v} = 60)$

The average and extreme values in Tables 5.5 and 5.6 refer to the average and extreme values assumed for the density of the soil.

5.4 Settlements

The theoretical settlements using the various values of the soil properties in Table 5.4 were calculated with the procedures explained in section 3.5.

Before the change in void ratio Δe could be obtained from the e:log P curve in Figure 5.9 it was necessary to estimate the approximate effective stress, ie

$$\sigma_y' = \sigma_y - \bar{u}_a$$

The average excess pore-air pressure $\bar{u}_a$ was obtained from the computer program explained in Chapter 4. This program produced average excess pore-air pressure in the central core of the embankment for each row between columns 108 through 113 of the finite difference grid in Figure 5.3 at the end of construction and at thirty two time intervals after completion. The duration of each time interval was approximately two months (ie sixteen time-steps of Δt = approximately half a week each).

As explained in section 3.5, the ultimate settlement of the crest is given by,

$$\delta = \delta_i + \delta_c$$

The immediate settlement δ_i was defined as the settlement that had already occurred by the end of construction. This settlement was estimated from the e:log P curve in Figure 5.9 after using the average excess pore-air pressures at the end of construction (obtained from the computer program) to

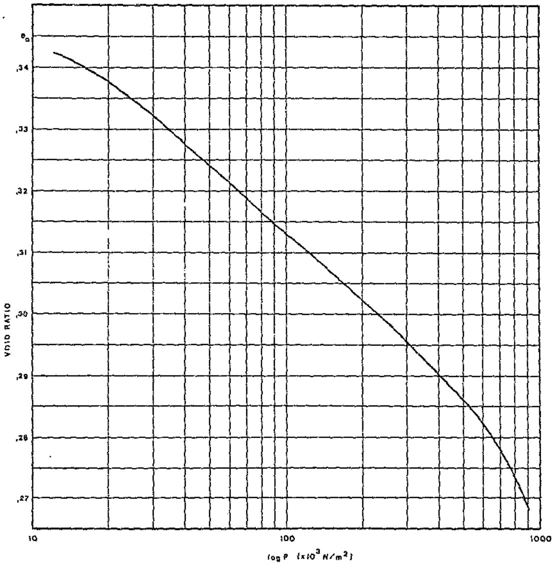

FIGURE 5.9

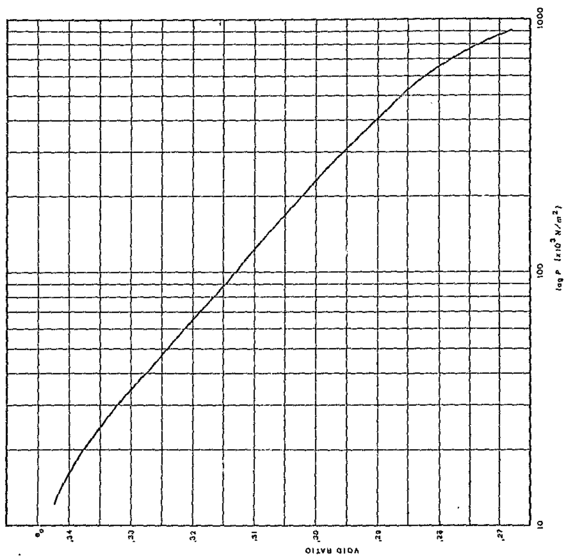

FIGURE 5.9

calculate effective stress in the different soil layers in the central core.

The consolidation settlement δ_c is the settlement that occurred after completion and is in excess of the immediate settlement. This settlement was calculated by first estimating the total settlement δ_t at a given time and then substracting the immediate settlement δ_i from it,

$$\delta_c = \delta_t - \delta_i$$

The ultimate settlement of the crest was calculated by assuming that the excess pore-air pressure in the central core had completely dissipated ie,

$$\sigma_y' = \sigma_y$$

Table 5.7 and Figure 5.10 present a summary of the calculated ultimate, immediate and consolidation settlements for the various values of the soil properties in Table 5.4 and a comparison between actual and calculated consolidation settlements are given in Figure 5.11.

TABLE 5.7

Calculated Settlements in Embankment Dam

$c_v = 10{,}5\ m^2/year$

$\Delta t = 0{,}013$ year

γ ($x10^3$ N/m^3)	B_a	immediate settlement (m)	consolidation settlement (m)	ultimate settlement (m)
22,1	0,65	1,587	0,533	2,120
22,1	0,75	1,441	0,679	2,120
22,1	0,80	1,393	0,727	2,120
22,6	0,90	1,231	0,908	2,139

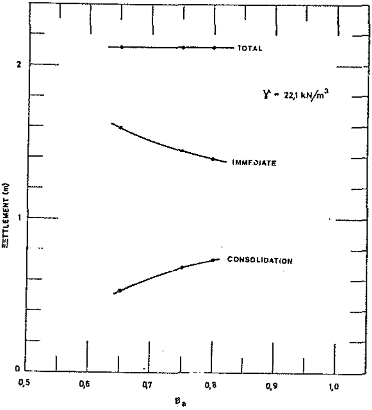

Figure 5.10

5.5 Discussion of Settlement Results

The theoretical settlement curves in Figure 5.11 indicate that higher initial pore-air pressures u_{ao} in the compacted soil increase the consolidation settlement δ_c of the embankment (curves II and III). Consolidation settlements calculated with pore-pressure coefficients determined by the *weighted column* method are also larger than those calculated with pore-pressure coefficients determined by the *weighted area* method. Curves I, II and III underestimate the consolidation settlement while curve V which was calculated by using extreme values for the soil properties overestimates settlement.

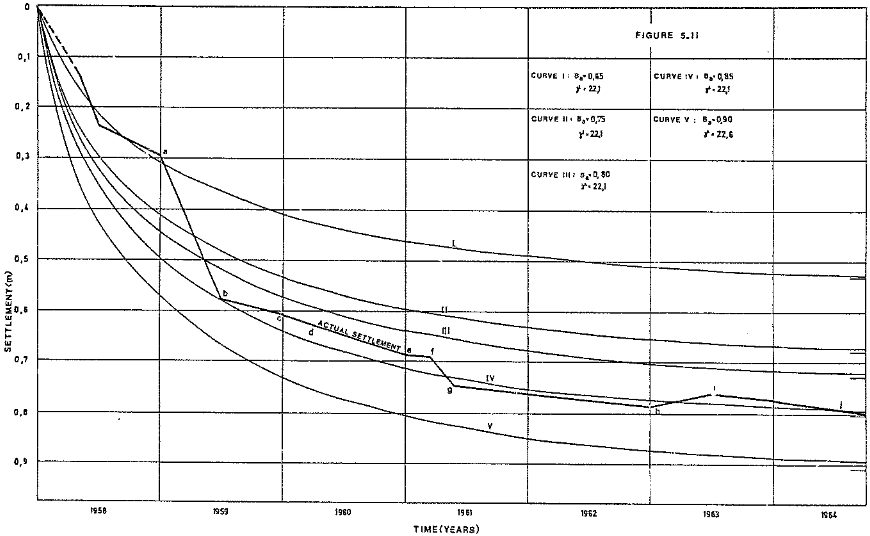
CURVE I : B_a = 0,65 γ' = 22,1
CURVE II : B_a = 0,75 γ' = 22,1
CURVE III : B_a = 0,80 γ' = 22,1
CURVE IV : B_a = 0,85 γ' = 22,1
CURVE V : B_a = 0,90 γ' = 22,6
ACTUAL SETTLEMENT
a
b
c
d
e
f
g
h
i
j
I
II
III
IV
V
SETTLEMENT (m)
0
0,1
0,2
0,3
0,4
0,5
0,6
0,7
0,8
0,9
1958
1959
1960
1961
1962
1963
1964
TIME (YEARS)

FIGURE 5.11

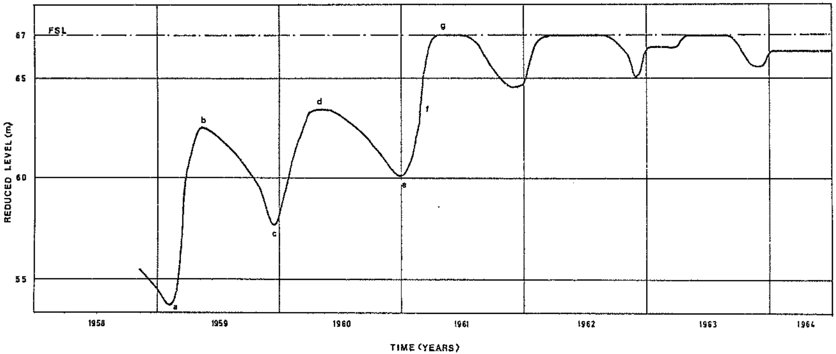

WATERLEVEL IN RESERVOIR

FIGURE 5.12

Not one of the theoretical settlement curves calculated with soil properties from Table 5.4 coincides with the measured settlement curve. It was consequently decided to determine by trial and error the value of the pore-pressure coefficient B_a that would make the two curves coincident. The best fit between theoretical and actual settlement curves were obtained for B_a = 0,85 (curve IV).

If the actual settlement curve in Figure 5.11 is studied in conjunction with the water level curve of the reservoir in Figure 5.12 some interesting relationships are noted. The sudden rises in water level over sections ab and fg were accompanied by sudden increases in settlement although there seems to be no significant increase in the rate of settlement over sections cd and ef where the water level also increased. If it is assumed that the additional water load had an effect on the settlement of the crest an explanation must be sought for the flatter slopes of sections cd and ef.

The increase in water level from a to b was the first significant additional loading imposed on the embankment. It would thus be reasonable to assume that the additional settlement could be calculated from the virgin line of the e:log P curve. The unloading from b to c caused a rebound in the settlement curve with the result that the additional settlement due to loading cd was governed by the overconsolidation part of the curve (see Figure 5.13).

The same argument applies to the unloading from d to e and reloading from e to f. The loading from f to g was again on the virgin line of the settlement curve as this loading had not occurred previously.

The slope of the e:log P curve over sections ab and fg is larger than over sections cd and ef which explains why the

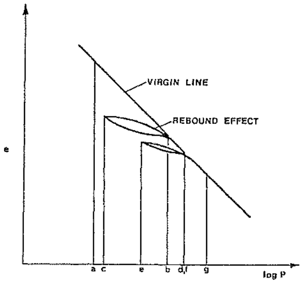

Figure 5.13

rate of settlement over sections ab and fg was larger than over sections cd and ef.

The above postulation will not be checked as the stress distribution in the central core due to the increased water load is unknown. The determination of this stress distribution is considered to be outside the scope of this dissertation.

It will be noticed that the points a,b,...,f,g do not occur at exactly the same times on the two graphs. The reason for this could be that the settlements were not determined at exactly the same time when the water level was at the different peaks. This would lead to a distorted observed time-settlement curve.

The rise in the settlement curve over section hij could be due to survey errors.

The instantaneous undrained compression due to the additional water load over section ab could have increased the degree of saturation of the soil which would have led to a higher value of B_a. A possible theoretical reconstruction of the actual settlement curve may be as presented in Figure 5.14 with the variable values of B_a as shown in Table 5.8.

TABLE 5.8

Time (years)	Best fit value of B_a
0 - 1	0,65
1 →	0,85

The maximum error in terms of ultimate settlement (immediate plus consolidation settlement) for the various assumptions used to calculate the curves in Figure 5.11 is 12 per cent. If the maximum error is expressed in terms of consolidation settlement, which is only a part of the complete settlement curve, it is found to be 34 per cent.

It is valuable to compare the accuracy stated above with that of other methods used to estimate settlements in embankments. One of the most popular methods used currently in geotechnical engineering is the finite element technique.

The finite element technique was used to estimate settlements in Oroville Dam. Duncan (1972) reported comparisons between actual and predicted ultimate settlements published by Kulhawy and Duncan (1970) and the accuracy was found to be approximately 25 per cent. Measured settlements were larger

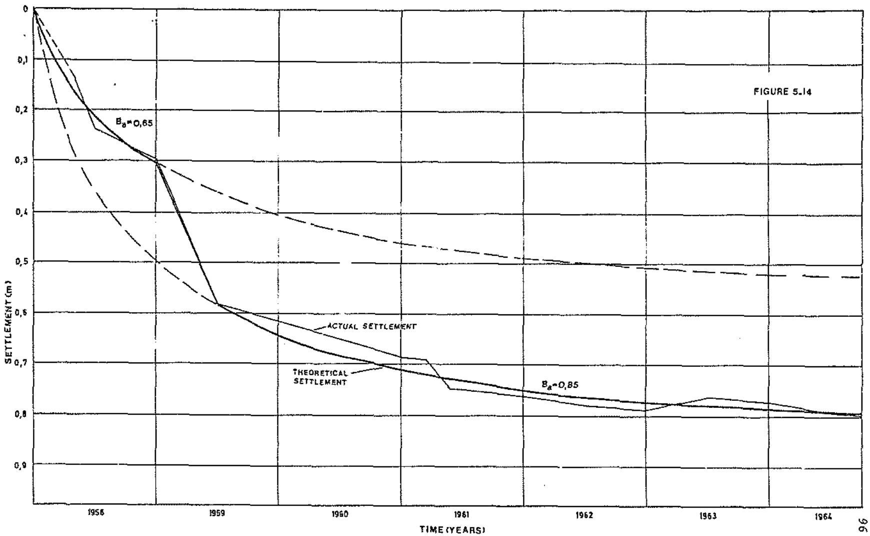

0
0,1
0,2
0,3
0,4
0,5
0,6
0,7
0,8
0,9
SETTLEMENT (m)
B_a=0,65
ACTUAL SETTLEMENT
THEORETICAL SETTLEMENT
B_a=0,85
1958
1959
1960
1961
1962
1963
1964
TIME (YEARS)

FIGURE 5.14

than predicted settlements. Duncan (1972) described the agreement as "quite good".

Duncan (1972) also reported findings of Nobari and Duncan (1972a,b) who performed a finite element analysis to determine movements in Oroville Dam caused by filling of the reservoir. Nobari and Duncan (1972a,b) ignored consolidation of the embankment due to its own weight in this analysis and it was found that the calculated vertical settlements were considerably smaller than the measured settlements. Duncan (1972) was of the opinion that the large difference was due to the effects of creep, secondary compression and consolidation which was not taken into account in the analysis. It can be concluded from this that the effect of water load on the settlement of the crest may be small.

Penman *et al* (1971) also compared observed settlements with settlements predicted by the finite element technique. Total settlements were measured at a large number of points throughout the embankment and errors varied between 0 per cent and 38 per cent.

From this comparison and discussion it can be concluded that the finite difference technique used in this dissertation in conjunction with oedometer data is of the same order of accuracy as other available methods and can confidently be used to estimate settlements of embankment dams.

The engineer must keep in mind that the water load may have an effect on the settlement of the crest and that the initial pore-air pressures in the compacted soil may be higher than atmospheric pressure. It would be advisable to measure initial pore-air pressures in compacted soil samples to enable a realistic assessment of B_a during the design stage to be made. The assumptions made in design can be checked by installing piezometers in the embankment to measure actual excess pore-air pressures during construction.

CHAPTER 6

REVIEW AND CONCLUSIONS

1. Bishop's effective stress equation was discussed and the conclusion was reached that effective stresses for volume change in unsaturated soil subjected to compression at constant water content are dependent on $(\sigma - u_a)$. The settlement curves obtained from oedometer tests for unsaturated soils are in terms of $(\sigma - u_a)$ with $u_a = 0$ and the suction $(u_a - u_w)$ and higher permeability of the soil to air are indirectly taken into account in the shape of the time settlement curve. Because u_a is always greater than u_w and because u_a dissipates to atmospheric pressure, consolidation in unsaturated soil is controlled by the dissipation of excess pore-air pressure. Water will not drain from an unsaturated soil unless it becomes saturated by compression.

2. The magnitude of the pore-air pressures in an embankment at the end of construction are dependent on the construction rate, soil properties (c_v, γ, B_a) and the geometry of the embankment. It was found that pore-air pressures at the end of construction are very sensitive to changes in soil density γ and the pore-pressure coefficient B_a and less sensitive to changes in the coefficient of consolidation c_v and the rate of construction.

3. The soil properties required to calculate excess pore-air pressures in unsaturated soil can be determined from oedometer test results.

The initial settlement in the consolidation curve for an unsaturated soil is much larger than that for a saturated soil. This is due to the higher air content of the soil and the higher compressibility of air. After the *corrected zero* for the unsaturated soil has been established correctly the *root time* method can be used to estimate realistic values of c_v.

It is possible to estimate excess pore-air pressures in unsaturated soil by combining Boyle's and Henry's laws. These pressures are dependent on the initial pore-air pressure set up in the soil during compaction. With a knowledge of the excess pore-air pressure under specified loading conditions it is possible to estimate the pore-pressure coefficient B_a. Higher initial pore-air pressures lead to higher values of B_a.

With a knowledge of the specific gravity of the soil it is possible to estimate soil density for different void ratios and degrees of saturation.

4. A differential equation was derived to estimate pore-air pressures in an embankment of unsaturated soil which increases in height with time,

$$\frac{\partial u_a}{\partial t} = c_v \left(\frac{\partial^2 u_a}{\partial x^2} + \frac{\partial^2 u_a}{\partial y^2}\right) + \gamma . B_a . \frac{\partial h}{\partial t}$$

This equation takes into account the soil properties, additional load added during construction, dissipation of excess pore-air pressure during construction, construction rate and geometry of the embankment.

By knowing the excess pore-air pressure in the embankment it is possible to estimate the independent variable portion of the effective stress,

$$\sigma' = \sigma - u_a$$

and hence the settlement from the e:log P curve obtained from oedometer tests.

5. A computer program has been developed to calculate excess pore-air pressures in embankments using the finite difference form of the differential equation given under 4. This program predicts pore-air pressures in embankments at the end of construction and also at certain time intervals after completion.

These excess pore-air pressures are used to estimate settlement.

6. The settlement of embankments constructed of unsaturated compacted soil is given by,

$$\delta = \delta_i + \delta_c$$

where

$$\delta_i = \delta_e + \delta_{inst} + \delta_{cons}$$

The shear deformation δ_e was ignored in this dissertation.

In the presented case study it was found that the settlement that occurred during construction δ_i was much larger than the consolidation settlement δ_c that occurred after completion.

Increased initial pore-air pressures set up in the soil during construction led to increased consolidation settlement δ_c.

It was concluded that the water load due to filling of the reservoir must have some effect (although of unknown magnitude) on the consolidation settlement δ_c. Studies by Nobari and Duncan (1972a,b) indicate that its contribution was small in the case of Oroville Dam. However, at Mita Hills, water load could have been responsible for 34 per cent of post-construction settlement.

7. By comparing observed and calculated settlements for Mita Hills Dam it was found that the maximum error in terms of ultimate settlement was 12 per cent. This accuracy is comparable with other techniques, notably the finite element technique.

It can thus be concluded that the finite difference technique presented in this dissertation in conjunction with soil properties obtained from oedometer test results can be used in practice to estimate settlements of the crests of embankments.

REFERENCES

1. Biot, M A, General Theory of Three-Dimensional Consolidation, *Journal of Applied Physics*, Vol 12 (1941)
2. Bishop, A W, The Use of Pore-Pressure Coefficients in Practice, *Geotechnique*, Vol 4 (1959)
3. Bishop, A W, The Principle of Effective Stress, *Tecknisk Ukeblad*, Number 39 (1959)
4. Bishop, A W, Some Factors Controlling the Pore Pressure set up during the Construction of Earth Dams, *Proceedings of the Fourth International Conference on Soil Mechanics*, London (1957)
5. Bishop, A W and Blight G E, Some Aspects of Effective Stress in Saturated and Partly Saturated Soils, *Geotechnique*, Number 13 (1963)
6. Bishop, A W and Donald, I B, The Experimental Study of Party Saturated Soils in the Triaxial Apparatus, *Proceedings of the Fifth International Conference on Soil Mechanics*, Vol I, Paris (1961)
7. Bishop, A W and Henkel, D J, *The Measurement of Soil Properties in the Triaxial Test*, Second Edition, London: Edward Arnold (1962)
8. Blight, G E, *Strength and Consolidation Characteristics of Compacted Soils*, PhD Thesis, London (1961)
9. Blight, G E, Controlling Earth-dam Compaction under Arid Conditions, *Civil Engineering* (1962)
10. Blight, G E, A Study of Effective Stress for Volume Change, *Symposium on Moisture Equilibria and Moisture Change in Soils beneath covered areas*, Butterworths, (Australia) (1965)

11. Blight, G E, The Utilisation of Soil Suction in the Design of Earth Dam Embankments, *Proceedings of the Third Regional Conference for Africa on Soil Mechanics and Foundation Engineering* (1963)

12. Blight, G E, Strength Characteristics of Dessicated Clays, *Journal of the Soil Mechanics and Foundations Division*, Proc ASCE, Vol 92, SM6, November (1966)

13. Blight, G E, Effective Stress Evaluation for Unsaturated Soils, *Journal of the Soil Mechanics and Foundations Division*, Proc ASCE, Vol 93, SM2, March (1967)

14. Blight, G E, Construction Pore Pressures in two Sloping-core Rockfill Dams, *Transactions of the Tenth International Congress on Large Dams*, Montreal, Canada (1970)

15. Brackley, I J A, *Inter-relationship of the Factors Affecting Heave of an Expansive, Unsaturated, Clay Soil*, PhD Thesis, University of Natal (1975)

16. Burland, J B, *The Concept of Effective Stress in Partly Saturated Soils*, MSc Thesis, University of the Witwatersrand (1961)

17. Burland, J B, Some Aspects of the Mechanical Behaviour of Partly Saturated Soils, *Symposium on Moisture Equilibria and Moisture Change in Soils Beneath covered areas*, Butterworths (Australia) (1965)

18. Carillo, N, Simple Two and Three Dimensional Cases in the Theory of Consolidation of Soils, *Journal of Mathematics and Physics*, Vol 21 (1942)

19. Cavounidis, S and Höeg, K, Consolidation During Construction of Earth Dams, *Journal of the Geotechnical Engineering Division*, Proceedings ASCE, Vol 103, GT10, October (1977)

20. Carnahan, B and Wilkes, J O, *Digital ing and Numerical Methods*, New York: John W & Sons (1973)

21. De Mello, V F B, Reflections on Design Decisions of Practical Significance to Embankment Dam, *Geotechnique*, Vol 27 (1977)

22. Desai, C S and Christian, J T, *Numerical Methods in Geotechnical Engineering*, New York: McGraw-Hill (1977)

23. Duncan, J M, Finite Element Analyses of Stresses and Movements in Dams, Excavations and Slopes, *Proceedings of the Symposium on Applications of the Finite Element Method in Geotechnical Engineering*, Vicksburg, Mississippi, U S Army Corps of Engineers (1972)

24. Fredlund, D G, Engineering Approach to Soil Continua, *Second Symposium on Applications of Solid Mechanics*, Hamilton, Ontario, Canada (1974)

25. Fredlund, D G and Morgenstern, N R, Constitutive Relations for Volume Change in Unsaturated Soils, *Canadian Geotechnical Journal*, Vol 13, Number 3 (1976)

26. Fredlund, D G, Density and Compressibility Characteristics of Air-Water Mixtures, *Canadian Geotechnical Journal*, Vol 13, Number 4 (1976)

27. Fredlund, D G and Morgenstern, N R, Stress State Variables for Unsaturated Soils, *Journal of the Geotechnical Engineering Division*, Proceedings ASCE, Vol 103, GT5, May (1977)

28. Gibson, R E, The Progress of Consolidation in a Clay Layer Increasing in Thickness with Time, *Geotechnique*, Vol 8 (1958)

29. Gibson, R E and Lumb, P, Numerical Solutions in some problems in the Consolidation of Clay, *Proceedings ICE*, Part 1, 2 (1953)

30. Hilf, J W, Estimating Construction Pore Pressures in Rolled Earth Dams, *Proceedings of the Second International Conference on Soil Mechanics and Foundation Engineering*, Vol 3 (1948)

31. Holtz, W G, The Determination of Limits for the Control of Placement Moisture in High Rolled-Earth Dams, *Proc ASCE*, Vol 48 (1948)

32. Jennings, J E B, A Revised Effective Stress Law for use in the Prediction of the Behaviour of Unsaturated Soils, *Pore Pressure and Suction in Soils*, London: Butterworths (1961)

33. Jennings, J E B and Burland, J B, Limitations to the Use of Effective Stresses in Partly Saturated Soils, *Geotechnique*, Vol 12 (1962)

34. Jennings, J E and Knight, K, A Guide to Construction on or with Materials Exhibiting Additional Settlement due to "Collapse" of Grain Structure, *Proceedings of the Sixth Regional Conference for Africa on Soil Mechanics and Foundation Engineering*, Durban, South Africa (1975)

35. Justin, J D, Hinds, J and Craeger, W P, *Engineering for Dams*, Fifth edition, Vol III, New York: John Wiley & Sons (1955)

36. Knight, K, *The Collapse of Structure of Sandy Sub-soils on Wetting*, PhD Thesis, University of the Witwatersrand (1961)

37. Kulhawy, F H and Duncan, J M, *Non-linear Finite Element Analysis of Stresses and Movements in Oroville Dam*, Geotechnical Engineering, University of California, Report no TE-70-2 (1970)

38. Lambe, T W and Whitman, R V, *Soil Mechanics*, New York: John Wiley and Sons (1969)

39. Lambe, T W, Stress Path Method, *Journal of the Soil Mechanics and Foundations Division*, Proceedings ASCE, Vol 93, SM6 (1967)

40. Legge, G H H, Mulungushi and Mita Hills Dams Operation and Maintenance, *Transactions of the Tenth International Congress on Large Dams*, Montreal, Canada (1970)

41. Li, C Y, Construction Pore Pressures in Three Earth Dams, *Journal of the Soil Mechanics and Foundations Division*, Proceedings ASCE, Vol 93, SM2 (1967)

42. Nobari, E S and Duncan, J M, *Effects of Reservoir Filling on Stresses and Movements in Earth and Rockfill Dams*, Geotechnical Engineering Report, University of California, Berkeley (1972a)

43. Nobari, E S and Duncan, J M, Movements in Dams due to Reservoir Fillings, *Proc of the ASCE Soil Mechanics and Foundations Speciality Conference on Performance of Earth and Earth-Supported Structures*, Purdue (1972b)

44. Olson, R E and Langfelder, L J, Pore Water Pressure in Unsaturated Soils, *Journal of the Soil Mechanics and Foundations Division*, Proceedings ASCE, Vol 91, SM4 (1965)

45. Penman, A D M, Burland, J B and Charles, J A, Observed and Predicted Deformations in a Large Embankment Dam During Construction, *Proceedings ICE*, Vol 49 (1971)

46. Sherman, W C and Clough, G W, Embankment Pore Pressures during Construction, *Journal of the Soil Mechanics and Foundations Division*, Proceedings, ASCE, Vol 94, MS2 (1968)

47. Skempton, A W, The Pore-Pressure Coefficients A and B, *Geotechnique*, Vol 4 (1954)

48. Schiffman, R L, Chen, A T F and Jordan, J C, An Analysis of Consolidation Theories, *Journal of the Soil Mechanics and Foundations Division*, Proceedings ASCE, Vol 95, SM1 (1969)

49. Scott, C R, *An Introduction to Soil Mechanics and Foundations*, Second edition, London: Applied Science Publishers (1974)

50. Taylor, D W, *Fundamentals of Soil Mechanics*, New York: John Wiley & Sons (1948)

51. Terzaghi, K, *Theoretical Soil Mechanics*, New York: John Wiley & Sons (1943)

52. Thomas, H H, *The Engineering of Large Dams*, London: John Wiley and Sons (1976)

53. Wagener, F, *Consolidation Settlement of Soils under Repetitive Loading as Experienced in Road Foundations*, MSc Thesis, University of the Witwatersrand (1960)

54. USBR, *Earth Manual*, Second edition, Washington: United States Government Printing Office (1974)

55. USBR, *Design of Small Dams*, Second edition, Washington: United States Government Printing Office (1973).

Author Annandale George William
Name of thesis Settlement Of Embankments Constructed Of Unsaturated Compacted Soil. 1979

PUBLISHER:
University of the Witwatersrand, Johannesburg
©2013

LEGAL NOTICES:

Copyright Notice: All materials on the University of the Witwatersrand, Johannesburg Library website are protected by South African copyright law and may not be distributed, transmitted, displayed, or otherwise published in any format, without the prior written permission of the copyright owner.

Disclaimer and Terms of Use: Provided that you maintain all copyright and other notices contained therein, you may download material (one machine readable copy and one print copy per page) for your personal and/or educational non-commercial use only.

The University of the Witwatersrand, Johannesburg, is not responsible for any errors or omissions and excludes any and all liability for any errors in or omissions from the information on the Library website.